Scaling Laws in Permeability and Thermoelasticity of Random Media

Xiangdong Du

Department of Mechanical Engineering
McGill University, Montreal
May, 2006

Thesis submitted to McGill University in partial fulfillment of
the requirements of the degree of Doctor of Philosophy
in Mechanical Engineering

Your file Votre référence
ISBN: 978-0-494-32174-4
Our file Notre référence
ISBN: 978-0-494-32174-4

Abstract

Under consideration is the finite-size scaling of two thermomechanical responses of random heterogeneous materials. Stochastic mechanics is applied here to the modeling of heterogeneous materials in order to construct the constitutive relations. Such relations (e.g. Hooke's Law in elasticity or Fourier's Law in heat transfer) are well-established under spatial homogeneity assumption of continuum mechanics, where the Representative Volume Element (RVE) is the fundamental concept. The key question is what is the size L of RVE? According to the *separation of scales* assumption, L must be bounded according to

$$d < L << L_{Macro}$$

where d is the microscale (or average size of heterogeneity), and L_{Macro} is the macroscale of a continuum mechanics problem. Statistically, for spatially ergodic heterogeneous materials, when the mesoscale is equal to or bigger than the scale of the RVE, the elements of the material can be considered homogenized. In order to attain the said homogenization, two conditions must be satisfied: (a) the microstructure's statistics must be spatially homogeneous and ergodic; and (b) the material's effective constitutive response must be the same under uniform boundary conditions of essential (Dirichlet) and natural (Neumann) types.

In the first part of this work, the finite-size scaling trend to RVE of the Darcy law for Stokesian flow is studied for the case of random porous media,

without invoking any periodic structure assumptions, but only assuming the microstructure's statistics to be spatially homogeneous and ergodic. By analogy to the existing methodology in thermomechanics of solid random media, the Hill-Mandel condition for the Darcy flow velocity and pressure gradient fields was first formulated. Under uniform essential and natural boundary conditions, two variational principles are developed based on minimum potential energy and complementary energy. Then, the partitioning method was applied, leading to scale dependent hierarchies on effective (RVE level) permeability. The proof shows that the ensemble average of permeability has an upper bound under essential boundary conditions and a lower bound under uniform natural boundary conditions.

To quantitatively assess the scaling convergence towards the RVE, these hierarchical trends were numerically obtained for various porosities of random disk systems, where the disk centers were generated by a planar Poisson process with inhibition. Overall, the results showed that the higher the density of random disks – or, equivalently, the narrower the micro-channels in the system – the smaller the size of RVE pertaining to the Darcy law.

In the second part of this work, the finite-size scaling of effective thermoelastic properties of random microstructures were considered from Statistical to Representative Volume Element (RVE). Similarly, under the assumption that the microstructure's statistics are spatially homogeneous and ergodic, the SVE is set-up on a mesoscale, i.e. any scale finite relative to the microstructural length scale. The Hill condition generalized to thermoelasticity

dictates uniform essential and natural boundary conditions, which, with the help of two variational principles, led to scale dependent hierarchies of mesoscale bounds on effective (RVE level) properties: thermal expansion strain coefficient and stress coefficient, effective stiffness, and specific heats. Due to the presence of a non-quadratic term in the energy formulas, the mesoscale bounds for the thermal expansion are more complicated than those for the stiffness tensor and the heat capacity. To quantitatively assess the scaling trend towards the RVE, the hierarchies are computed for a planar matrix-inclusion composite, with inclusions (of circular disk shape) located at points of a planar, hard-core Poisson point field. Overall, while the RVE is attained exactly on scales infinitely large relative to microscale, depending on the microstructural parameters, the random fluctuations in the SVE response become very weak on scales an order of magnitude larger than the microscale, thus already approximating the RVE.

Based on the above studies, further work on homogenization of heterogeneous materials is outlined at the end of the thesis.

Keywords: Representative Volume Element (RVE), heterogeneous media, permeability, thermal expansion, mesoscale, microstructure.

Résumé

L'échelonnage de taille finie de la réponse mécanique effective des matériaux hétérogènes aléatoires est considéré ici. La mécanique stochastique est appliquée pour la modélisation des matériaux hétérogènes afin de former les relations constitutives telles que la loi de Hooke en élasticité ou la loi de Fourier en transfert thermique. Dans la mécanique stochastique, l'élément volumique représentatif (RVE) est un concept important et est considéré comme une propriété globale des matériaux hétérogènes. L'élément statistique de volume (SVE) est ajusté la mésoéchelle, laquelle se trouve,

$$d < L << L_{Macro}$$

où L est la mésoéchelle, d est la micro-échelle ou la taille moyenne de l'hétérogénéité, et L_{Macro} est la macro-échelle. Statistiquement, pour les matériaux hétérogènes ergodiques dans l'espace, quand la mésoéchelle est égale ou plus grande que l'échelle du RVE, les éléments du matériau peuvent être considérés comme étant homogénéisés. Afin d'atteindre ladite homogénéisation, deux conditions doivent être satisfaites : (a) les statistiques de la microstructure doivent être homogènes et ergodiques dans l'espace ; et (b) la réponse constitutive effective du matériau doit être identique sous les conditions limites uniformes de type essentiel (Dirichlet) et naturel (de Neumann).

Dans la première partie de ce travail, la tendance de l'échelonnage de taille finie du RVE de la loi de Darcy pour l'écoulement de Stokes a été étudiée pour le cas des milieux poreux aléatoires sans faire appel à aucune hypothèse sur la structure périodique, mais en assumant uniquement que les statistiques de la microstructure sont homogènes et ergodiques dans l'espace. Par analogie à la méthodologie existante en thermomécanique pour les milieux aléatoires solides, la condition de Hill-Mandel pour la vitesse d'écoulement de Darcy et des champs de gradient de pression a été initialement formulée. Sous les conditions limites essentielles et naturelles, deux principes variationnels ont été développés basé sur l'énergie potentielle minimum et l'énergie complémentaire. Ensuite, la méthode de division a été appliquée, menant à mesurer des hiérarchies dépendantes par rapport à la perméabilité effective (au niveau du RVE). La preuve démontre que la moyenne d'ensemble de perméabilité a une limite supérieure sous les conditions limites essentielles et une limite inférieure sous les conditions limites uniformes.

Pour évaluer quantitativement la convergence de graduation vers le RVE, ces tendances hiérarchiques ont été obtenues numériquement pour des systèmes de disques aléatoires ayant différentes porosités, où les centres des disques ont été créés par un procédé planaire de Poisson utilisant l'inhibition. De façon générale, les résultats ont démontré que plus la densité des disques aléatoires est élevée - ou, d'une manière équivalente, que les micro-canaux dans le système sont étroits - plus petite est la taille du RVE selon la loi de Darcy.

Dans la deuxième partie de ce travail, l'échelonnage de taille finie des propriétés thermoélastiques effectives des microstructures aléatoires ont été considérées à

partir des éléments statistiques jusqu'aux éléments volumiques (RVE). De même, selon l'hypothèse que les données statistiques de la microstructure sont homogènes et ergodiques dans l'espace, le SVE est mesuré sur une mésoéchelle, c'est-à-dire n'importe quelle échelle finie relative à l'échelle microstructurale de longueur. La condition de Hill généralisée en thermoélasticité prescrit des conditions limites essentielles et naturelles uniformes, qui, avec l'aide de deux principes variationnels, ont mené à mesurer des hiérarchies dépendantes des limites de la mésoéchelle pour les propriétés effectives (au niveau du RVE) : le coefficient de déformation pour la dilatation thermique et le coefficient de contrainte, la rigidité effective, ainsi que les chaleurs spécifiques. En raison de la présence d'un terme non-quadratique dans les équations d'énergie, les limites de la mésoéchelle pour la dilatation thermique sont plus complexes que celles de la rigidité tensorielle et la capacité thermique. Pour évaluer quantitativement la tendance de graduation vers le RVE, les hiérarchies ont été calculées pour un composite planaire avec inclusions dans la matrice, avec des inclusions (en forme de disque circulaire) situées aux points d'un champ de Poisson planaire et endurci. De façon générale, alors que le RVE est atteint avec exactitude sur des échelles infiniment grandes relativement à la micro-échelle, selon les paramètres microstructuraux, les fluctuations aléatoires dans la réponse du SVE peuvent devenir très faibles sur les échelles ayant un ordre de grandeur plus important que la micro-échelle, de ce fait, approximant déjà le RVE.

Basé sur les études ci-dessus, une méthodologie de l'homogénéisation des matériaux hétérogènes a été déterminée à la fin de la présente recherche.

Mots-clés : Élément volumique représentatif (RVE), milieu hétérogène, perméabilité, dilatation thermique, mésoéchelle, microstructure.

Acknowledgement

I would like to express my sincerest gratitude to my supervisor, Professor Ostoja-Starzewski. I thank him for his inspiring guidance that led me to this magnificent field. Without his supervision, this work would not have been possible.

I also would like to thank my colleagues, Zemfira Khisaeva, Wei Li, Shivakumar Iyer and Dr. Ge Wang for their helpful discussions about this work.

Finally, I wish to thank my family, and especially my dear wife Yan Zeng, for their prolonged understanding, support and encouragement during the course of this work.

Table of Contents

Nomenclature

L: mesoscale (window size, element size) of heterogeneous medium ($[m]$);

d: Microscale ($[m]$);

L_{Macro}: macroscale ($[m]$);

δ : Nondimensional window size;

$\vec{U}$: Darcy Velocity ($[m/s]$);

K_{ij} or $\underline{K}$: the permeability tensor of the porous medium ($[m^2]$);

R_{ij} or $\underline{R}$: the resistance tensor of the porous medium ($[1/m^2]$);

μ : fluid viscosity ($[Pa \cdot s]$);

∇p : Pressure gradient ($[Pa/m]$);

$g(x)$: Source/sink term in Darcy equation ($[1/s]$);

$\vec{v}$: Actual fluid velocity in void region in porous media ($[m/s]$);

V_f : Void region in porous media;

$\sigma_{ij}(\vec{x})$: Stress on fluid particles ($[Pa]$);

$\tilde{\sigma}_{ij}(\vec{x})$: Trial stress on fluid particles ($[Pa]$);

$\tilde{p}(\vec{x})$: Trial pressure field (scalar function, $[Pa]$);

V : Medium domain or sample element;

∂V : Boundary on domain or sample element;

ϕ: Energy dissipation rate of porous media ($[J/m^3 \cdot s]$);

ϕ^P : Potential energy in terms of energy dissipation rate ($[J/m^3 \cdot s]$);

ϕ^C : Complementary energy in terms of energy dissipation rate ($[J/m^3 \cdot s]$);

$\vec{n}$: Unit normal vector of a surface element dS;

$\vec{x}$: Coordinate of dS;

$B(\omega)$: Random material realizations, a domain given unrestricted boundary condition;

$B^s_{\delta'}(\omega)$: Random material realizations, a domain given restricted boundary condition;

$\langle F(\vec{x}) \rangle$: Ensemble average over function $F(\vec{x})$;

σ_{ij} and $\underline{\sigma}$: Stress tensor ($[Pa]$);

ε_{ij} and $\underline{\varepsilon}$: Strain tensor;

C_{ijkl} and $\underline{\underline{C}}$: Stiffness tensor ($[Pa]$);

S_{ijkl} and $\underline{\underline{S}}$: Compliance tensor ($[1/Pa]$);

Γ_{ij} and $\underline{\Gamma}$: Thermal stress coefficient tensor ($[Pa/K]$);

α_{ij} and $\underline{\alpha}$:Thermal strain coefficient tensor ($[1/K]$);

P_{klmn} : Transformation tensor;

I_{klij} : Identity tensor;

κ : Bulk modulus ($[Pa]$);

Superscripts:

i: Inclusion.

m: Matrix

* : Effective properties

List of Figures

List of Tables

Chapter 1

Introduction

Deterministic continuum mechanics is based on the assumption of the existence of the Representative Volume Element (RVE). The classical continuum theories usually suggest that the infinitesimal elements are homogeneous such that the materials consisting of such elements are considered homogeneous. The theories and constitutive laws of modeling are well-established mathematically in mechanical engineering on homogeneous materials. However, the concept 'homogeneous' only exists in theory. All materials have some heterogeneity at certain scales or proportions. It has been noticed that the heterogeneous nature affects the accuracy of the analytical solutions of engineering problems. Hence, studies on the effects of heterogeneity are of great importance in many disciplines. Furthermore, with the development and application of composite materials, the effects of heterogeneity on materials become essential and raise many interesting research topics.

In most research and engineering applications, the detailed response of microstructures in heterogeneous materials is not necessarily known, and in some cases may not even be possible to determine. Macro-responses of heterogeneous media have, therefore, received considerable attention in the past several decades. In order to apply deterministic continuum mechanics on heterogeneous materials, many homogenization theories have been developed by researchers. When the homogenization of a heterogeneous material is considered, the shape, size and

properties of the microstructure in the materials need to be taken into account. It is commonly assumed that

$$d << L << L_{Macro} \tag{1.1}$$

where, L is the RVE size or separation scale, d is the microscale or average size of heterogeneity, and L_{Macro} is the macroscale. L is assumed 10 to 100 times bigger than d in most studies, often without being explicitly defined as such.

There still are some open questions, especially when attempting to formulate a solution to the governing partial differential equations. First, does the RVE preserve the properties which make the deterministic continuum theories applicable on heterogeneous materials? Also, what mechanical conditions (or modeling assumptions) are needed to ensure that the RVE is attained for heterogeneous materials? Most importantly, what is the scale of the RVE and how can the RVE scale for different physical phenomena be determined?

Many approaches to and topics on homogenization theory have been discussed thoroughly in the book by Torquato, S. (2002). Also, difference methods are comprehensively presented by Nemat-Nasser and Hori (1993).

The approaches can be catalogued into a number of categories, as follows: (i) rigorous energy bounds (e.g., of Hashin-Shtrikman type), (ii) perturbation methods (e.g. Beran, 1969), (iii) effective medium models, (iv) computational methods (e.g. Kanit et. al. 2003), and (v) asymptotic mesoscale bounds. Beginning in the late 1980s, a fifth approach to the determination of structure-property relations has been introduced and developed using bounds that explicitly

involve (a) the size of a mesoscale domain relative to the microscale, and (b) the type of boundary conditions applied to this domain (Huet, 1990; Sab, 1992). This fifth approach, that we here forth call it asymptotic bounds approach, was also driven by the need to derive continuum random field models of heterogeneous materials from actual microstructures (Ostoja-Starzewski & Wang, 1989; Ostoja-Starzewski, 1990, 1994, 1998). The effective properties (or the bounds of effective properties) can be determined by this approach as well.

In this thesis, two topics – permeability of porous media flow and thermal expansion of heterogeneous materials will be discussed. We hereby give two brief reviews on the previous work on these two topics respectively.

A. Flow in Porous Media – Permeability:

Fluid flows in porous media are important transport phenomena that are encountered in many engineering branches, such as filtration, oil recovery, soil hydrology etc. During the past several decades, various aspects of porous media flow have been extensively studied. Due to the heterogeneous nature of most porous materials, many difficulties and complexities arise in mathematic formulation and modeling. Numerous attempts to incorporate the permeability K with the microstructure (i.e. the pore geometry) have been made, including stochastic approaches (Zhang, 2001). Most applicable approaches in engineering applications are based on homogenization and RVE concept (Jacob Bear, 1988; Torquato, 2002).

As stated above, in order to overcome these uncertainties caused by randomness without going into detailed microstructure, finding rigorous bounds

of homogenized (effective) permeability has become one of the most important approaches (Weissberg and Prager, 1962; Berryman & Milton, 1985; Beasley & Torquato, 1988; Rubinstein and Torquato, 1989). Different variational principles were derived or applied by these authors. The inequalities of permeability, based on these variational principles were established, and the bounds were obtained. In these works, different assumptions were made on the results so that more rigorous bounds were established. Another approach was to use the effective medium theory that studies diluted and randomly arranged spheres (Childress, 1972; Howells, 1974). Often in effective medium approximations, idealized periodic structures of materials were studied (Zick and Homsy, 1982; Poutet, et. al. 1996; Kitanidis and Dykaar, 1997; Koch and Ladd, 1997). Computational approaches have also been applied in studies in porous media flows (Martys, 1994; Adler, et. al., 1990; Hill and Koch, 2001). Flows in the void region of porous media are simulated directly by different numerical methods. Averaged velocity of fluid is used to compute permeability.

In these aforementioned approaches, the scale dependence and boundary condition dependence of permeability were not discussed. In the present study, the asymptotic bounds approach is, for the first time, applied in studying the scale dependent bounds and the size of RVE in the permeability property of porous media flow. The detailed discussions are addressed in Chapter 2 of this thesis.

B. Thermal Expansion:

Thermal expansion is an important issue in mechanical engineering applications. Thermal deformation is considered as an eigenstrain (Love, 1926;

Mura, 1987). In the study of heterogeneous materials, homogenization is ~~also~~ the most important method in engineering applications and RVE is the central concept of homogenization (Markov, 2000; Nadeau and Ferrari, 2004). Thermal expansion response is coupled with elastic response and temperature change. Therefore, thermal expansion has a unique presence in the constitutive equations (Christensen, 1979). However, the similar approaches described above have been applied in seeking the effective thermal expansion coefficients of heterogeneous materials. Deriving variational principles and introducing rigorous bounds are of great use among these approaches (Shapery, 1968; Rosen and Hashin, 1970; Christensen, 1979). On the other hand, based on a pioneer work on the exact solution of elliptical micro-inclusion (Eshelby, 1957), the effective medium method was applied to estimate the effective thermal expansion coefficient (Markov, 2000). Numerical simulations were also preformed to obtain the thermal expansion properties of heterogeneous material (Sigmund and Torquato, 1996; Cheng and Batra, 2000).

Here we extend the asymptotic approach to study the scale dependence of thermal expansion properties. In Chapter 3, the detailed derivation and numerical results are discussed.

In asymptotic bounds approach, the topics below will be elaborated and discussed in order to develop the necessary foundation to obtain the asymptotic bounds for heterogeneous materials.

1.1 Ergodic Hypothesis

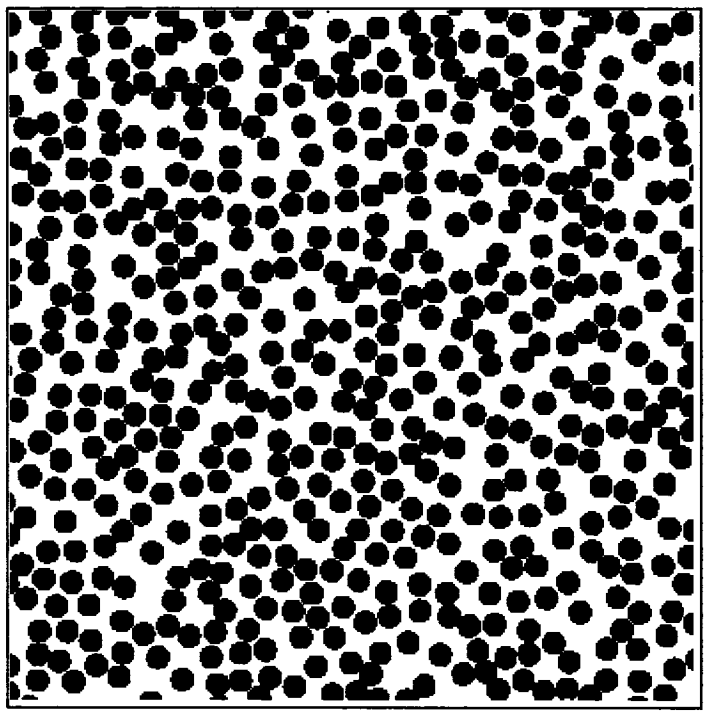

Figure 1-1 A computer generated field of media (random material) model.

The random heterogeneous materials, which are eligible to be homogenized, must be spatially stationary, or statistically homogeneous. In stochastic mechanics, a set of realization B is defined for a sample space Ω, such that $B=\{B(\omega);\omega\in\Omega\}$. The definition for statistically homogeneous can be expressed as,

$$P\{I^{(i)}(\mathbf{x}_1)=j_1,\cdots,I^{(i)}(\mathbf{x}_n)=j_n\}=P\{I^{(i)}(\mathbf{x}_1+\mathbf{y})=j_1,\cdots,I^{(i)}(\mathbf{x}_n+\mathbf{y})=j_n\} \quad (1.2)$$

where P is the probability function for a random space $B(\omega)$. $I^{(i)}(\mathbf{x}_n)$ is an indicator function for phase i, $\mathbf{x}_n\in B(\omega)$, and $\mathbf{y}$ is a constant vector. This

indicates that the different phases in materials are randomly distributed without preferred location or direction. Figure 1-1 shows a computer-generated random sample field in which this statistical homogeneity property is inherent.

The ergodic hypothesis states that the ensemble average over all realizations is equivalent to the spatial average over an infinite-volume, or

$$\overline{F(\omega)} \equiv \lim_{V\to\infty} \frac{1}{V} \int F(\vec{x},\omega) dv = \int_{\Omega} F(\vec{x},\omega) dP(\omega) \equiv \langle F(\vec{x}) \rangle \tag{1.3}$$

where $\langle \bullet \rangle$ denotes the ensemble average, and $P(\omega)$ is the probability distribution on Ω. $F(\vec{x},\omega)$ can be any function related to the phases, including the material properties. The ergodicity and its application are discussed by Torquato (2000) and Jeulin & Ostoja-Starzewski (2001).

The condition of ergodicity is a prerequisite for the application of the asymptotic mesoscale bounds to homogenization of heterogeneous materials.

1.2 Separation Scale

The left-hand side inequality in Equation 1.1 states that the RVE must be much greater than the characteristic length of the microstructures. However, recent studies (Ostoja-Starzewski 1998, 2005, 2006) show that d need not necessarily be orders of magnitude smaller than L. The separation scale is therefore proposed in a more complete form as

$$\left.\begin{matrix} d < \\ d << \end{matrix}\right\} L << L_{Macro} \tag{1.4}$$

The concept of the inequality in Equation 1.2 is demonstrated in Fig. 1-2. In a statistical sense, one may see that when the element is large enough to include considerable random structures, the effects of the microstructure may emerge and the macroscopic response becomes the same or similar.

Because the size of the heterogeneities varies in different materials, an important concept in the present study is introduced — nondimensional window (or element) size, which is defined as (Fig. 1-3)

$$\delta = \frac{L}{d} \tag{1.5}$$

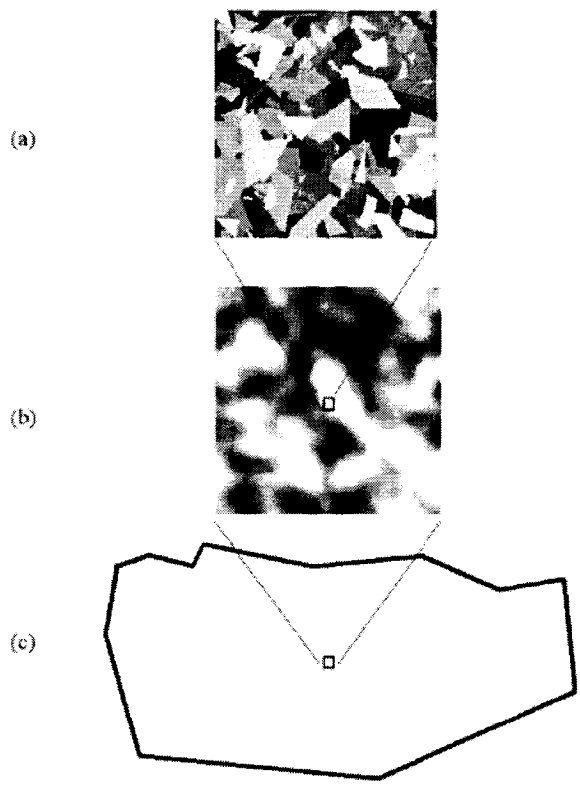

Figure 1-2 Three scales – micro (a), meso (b), and macro (c) - and randomness (after Ostoja-Starzewski 2001)

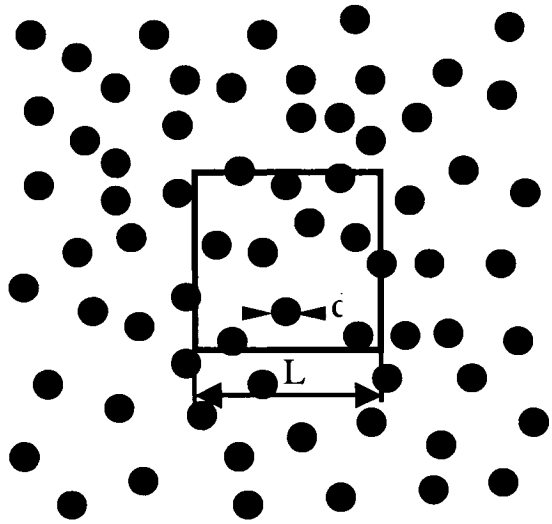

Figure 1-3 window scale vs. microscale

In Fig. 1-4 (a) and (b), two different realizations for $\delta = 2$ are shown, where the white phase is considered as matrix and the black phase as inclusions. It is apparent that the average properties of the two phases are different. However, in Fig. 1-1 in which $\delta = 32$, a change in the location of the inclusions may not cause a significant difference in apparent properties. This interpretation is prescribed by the following mathematic definitions.

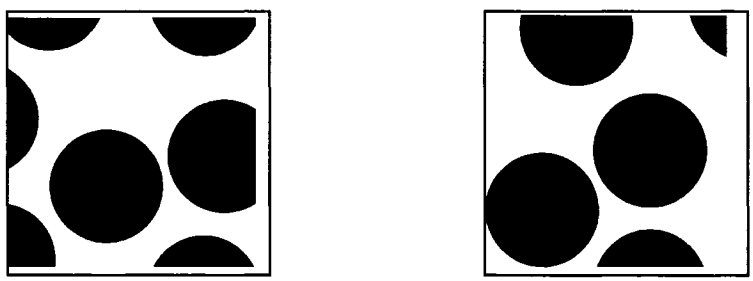

Figure 1-4 two realization of element size at $\delta = 2$

The RVE is clearly defined in either one of two situations: (i), a unit cell in a periodic microstructure, or (ii), a domain in a random medium, containing a very

large set of constituents, having statistically homogeneous and ergodic properties (Ostoja-Starzewski, 2005). The periodic microstructures are only relevant to theoretical solutions and numerical references, as no real engineering material can be ideally periodic. Therefore, case (ii) is the main focus in most homogenization studies.

When the periodicity of microstructure is not assumed, the definition of RVE is given by the pioneering work of Hill (1963), which defines the RVE as any sample which satisfies the following two conditions: (a) the sample is structurally entirely typical of the whole mixture on average, and (b) it contains a sufficient number of inclusions for the apparent overall moduli to be effectively independent of the surface values of traction and displacement, providing that these values are macroscopically uniform. The logic of Hill regarding the RVE was restated by Ostoja-Starzewski (1994, 2005) as follows:

(i) the microstructure's statistics must be spatially homogeneous and ergodic;

(ii) the material's effective constitutive response must be the same under uniform boundary conditions, of either the traction or displacement type.

In stochastic mechanics, the conceptual statistical volume element (SVE) is often used to model random heterogeneous materials. The size of the SVE is defined as the 'mesoscale', and the overall properties of the SVE are defined as the 'apparent' properties (Huet 1991). As the size of the mesoscale domain increases,

the quantification of the tendency to approach asymptotically from the SVE to the RVE in the sense of Hill (1963) is of great practical interest.

1.3 Bounds and Effective Properties:

Finding bounds is a common way to estimate the material properties when the exact value is difficult to determine. Due to the complexity and uncertainty of heterogeneous materials, most homogenization theories provide a method to determine the bounds of effective properties. Various physical phenomena, such as elastic moduli, conductivity, and permeability, have been studied (Torquato 2002, Markov & Preziosi, 2000, Nemat-Nasser & Hori, 1993). With the development of the homogenization theories, the more rigorous bounds are proved.

Nevertheless, these theories do not indicate how to obtain the size of the RVE, or on the other hand to study the apparent property tendency of the SVE with respect to increasing element scale. The asymptotic bound approach has the unique advantage of allowing for the study of scale dependency. In view of Hill's definition, the scale dependent bounds on the apparent stiffness tensor and the compliance tensor have been obtained under the essential (displacement) boundary and natural (traction) boundary conditions, respectively (Huet 1990, Wang & Ostoja-Starzewski 1989, Nemat-Nasser & Hori 1993). The completed form can be given as follows (Ostoja-Starzewski 1998),

$$\left\langle \underline{\underline{S}}^{t} \right\rangle^{-1} \leq \cdots \leq \left\langle \underline{\underline{S}}^{t}_{\delta} \right\rangle^{-1} \leq \left\langle \underline{\underline{S}}^{t}_{2\delta} \right\rangle^{-1} \leq \left\langle \underline{\underline{S}}^{t}_{4\delta} \right\rangle^{-1} \leq \cdots \leq (\underline{\underline{S}}^{*})^{-1} = \underline{\underline{C}}^{*} \leq \cdots$$

$$\cdots \leq \left\langle \underline{\underline{C}}^{d}_{4\delta} \right\rangle \leq \left\langle \underline{\underline{C}}^{d}_{2\delta} \right\rangle \leq \left\langle \underline{\underline{C}}^{d}_{\delta} \right\rangle \leq \cdots \leq \left\langle \underline{\underline{C}}^{d}_{n1} \right\rangle \qquad (1.5)$$

$\left\langle \underline{\underline{S}}^{t}_{\delta} \right\rangle$ is the ensemble average of compliance tensor at mesoscale δ under the traction (natural) boundary condition, and $\left\langle \underline{\underline{C}}^{n}_{\delta} \right\rangle$ is the ensemble average of stiffness tensor at mesoscale δ under the displacement (essential) boundary condition. The inequality relation between tensors in (1.5) means that, when $\underline{t} : \underline{\underline{A}} : \underline{t} \leq \underline{t} : \underline{\underline{B}} : \underline{t}$ for any $\vec{t}$, then $\underline{\underline{A}} \leq \underline{\underline{B}}$. This definition of tensor inequality is used though this thesis for both first- and second-order tensors. The scale dependent hierarchy expressed in Equation (1.5) reveals the following:

(i) To be considered as effective, the material must be macroscopically homogeneous such that in elasticity $(\overline{\overline{S}}^{*})^{-1} = \overline{\overline{C}}^{*}$.

(ii) The effective stiffness in linear elasticity is bounded from above under the displacement boundary condition and from below under the traction boundary condition.

(iii) The upper bound and lower bound converge toward effective stiffness as the mesoscale of the samples increases.

Note here the bounds are obtained from the ensemble average.

In the same paper (Ostoja-Starzewski 1998), the numerical simulation results for the material model with disk and needle inclusions randomly distributed show the convergence trend for the elastic stiffness tensor. The continuous results are also presented in Ostoja-Starzewski (1999) for random needles and cracks. Fig. 1-3 shows the numerical results and the convergence

trend of mesoscale bounds toward the effective response with the increasing mesoscale.

The numerical results also provide the convergence rate and discrepancy of the apparent stiffness tensor. Two general conclusions that have been made about the convergence of mesoscale domains to the RVE in the case of linear elastic microstructures are: (i) the situation of soft inclusions in a stiff matrix converges much more slowly with increasing size to RVE than the situation of stiff inclusions in a soft matrix; and (ii) the convergence of the anti-plane elasticity is slowest, while the in-plane elasticity converges more quickly, and the three-dimensional elasticity exhibits the most rapid convergence.

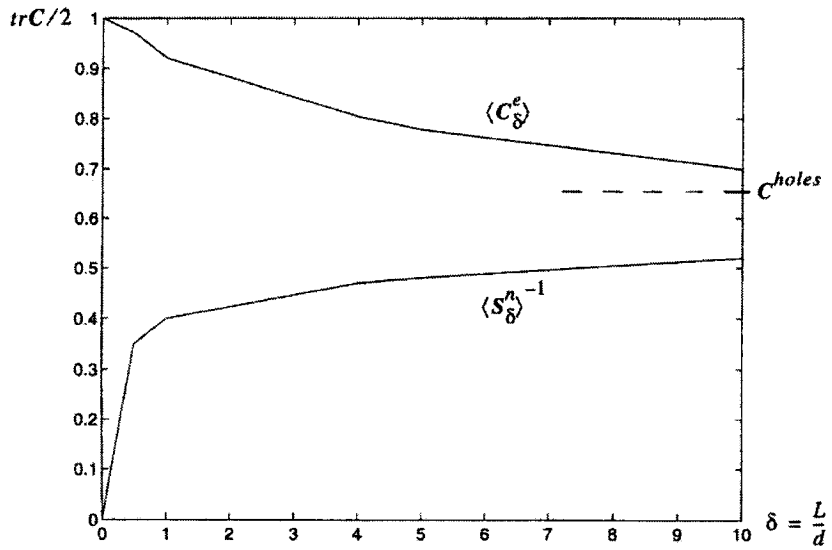

Figure 1-3 Effect of increasing mesoscale on the convergence of the hierarchy of scale dependent bounds for the composite (after Ostoja-Starzewski 1999).

This methodology was also applied to different mechanical or physical properties of heterogeneous materials, as will be discussed in the following section.

1.4 Phenomena and Objectives

The studies applying the asymptotic bound approach continue to be applied to different physical and mechanical fields. In linear elasticity, the hierarchical relation (1.5) has been studied and applied to different heterogeneous material models (Hill 1963; Huet 1990; Ostoja-Starzewski 1990, 1998, Nemat-Hori 1993).

In the work by Ostoja-Starzewski and Schulte (1996), the asymptotic mesoscale approach was applied to heat transfer (thermal conductivity) in heterogeneous materials. The mesoscale bounds (upper and lower) of effective thermal conductivities were proved by applying essential and natural boundary conditions, and demonstrated by numerical simulations.

Viscoelasticity is a more complex mechanical phenomenon. With a slight and novel modification of the asymptotic approach, theoretical bounds and size-effect hierarchies of the statistical viscoelastic stiffness and compliance function tensors were derived. Scale effects in plasticity are another challenging topic (Jiang & Ostoja-Starzewski 2001). Following the formulation of variational principles, the hierarchical bounds have been derived and the numerical simulation demonstrated the scale dependent bounds for rigid-perfectly-plastic materials. Also, a novel method by geodesic analysis was applied to study the plastic zone in which the energy principle is inherent (Ostoja-Starzewski 2005). Later work (Li & Ostoja-Starzewski 2005) has shown similar mesoscale bounds

on elastic-plastic (hardening) heterogeneous materials by means of numerical simulation. Recent work by Khisaeva & Ostoja-Starzewski (2006) applied this bounding method to non-linear (finite) elasticity.

In the present research, two new topics in thermomechanics of random media are discussed: the first is the flow in porous media, and the second is the thermal expansion in linear thermoelasticity. The thermomechanics is understood here in the broad and fundamental sense as the discipline of continuum mechanics and thermodynamics, which serves as the basis for derivation of a very wide range of constitutive equations of fluids and solids (Ziegler, 1983; Ziegler & Wehrli, 1987).

The objectives of this study are to determine the asymptotic mesoscale bounds on (i) the permeability tensor of random porous media and (ii) the thermal expansion coefficients (strain and stress), in order to carry out the homogenization procedure on the flow in porous media and in linear thermoelasticity, respectively.

Before getting into particular topics, an important point of this study should be made. With the rise of the computational methods and techniques in recent years, the finite element method has become the most useful means of solving engineering problems. The size of the finite elements must be larger than, at least equal to the size of the RVE for heterogeneous materials. The determination of the size of the RVE is critical to the accurate modeling of both engineering problems in both research areas. Refining mesh sometime may not be practical.

Chapter 2

On the size of representative volume element for Darcy law in random media[1]

2.1 Introduction

In this chapter we consider a steady, single-phase Stokesian fluid flow in random porous media with explicit account of a spatially disordered microstructure. In phenomenological, deterministic continuum mechanics, such a flow is described by Darcy's law (1856). With the slow flow in a porous medium also considered as incompressible and viscous, Darcy's law is governed by the equations (Dullien, 1979):

$$\vec{U} = -\frac{\underline{\underline{K}}}{\mu} \cdot \nabla p \tag{2.1.1}$$

$$\nabla \cdot \vec{U} = g(x) \tag{2.1.2}$$

where $\vec{U}$ is the Darcy (volume averaged) velocity ($[m/s]$), ∇p is the applied pressure gradient driving the flow ($[Pa/m]$), μ is the fluid viscosity ($[Pa \cdot s]$), and $\underline{\underline{K}}$ is the permeability ($[m^2]$), a second-rank tensor which depends on the microstructure of the porous medium. Equation (2.1.2) is the continuity equation

[1] Most of this chapter has been published as an article in *Proceedings of the Royal Society, London A., 2006*

wherein $g(x)$ is the source/sink term ($[1/s]$). The tensor $\underline{K}$ is usually considered a material property since it definitely depends on the porous microstructure. [In this chapter we interchangeably use the symbolic notation for 1st and 2nd rank tensors $\vec{a}$ and $\underline{b}$ or indicial notations a_i and b_{ij}, whichever is more convenient.]

Most studies on flow in random heterogeneous media are based on the assumption of the existence of an RVE, and are focused on the properties of the RVE without quantitatively specifying its size L relative to that of the micro-heterogeneity d, e.g. (Berryman and Milton, 1985; Nemat-Nasser & Hori, 1999; Torquato 2002), as mentioned in the last chapter.

More specifically, the RVE is taken to satisfy the so-called 'separation of scales' L. As seen in (1.2), the right-side inequality ensures the applicability of continuum mechanics with Darcy's law as the constitutive relation governing the response of the RVE. However, the left-side inequality in (1.2) is postulated rather vaguely (and sometimes involving $d << L$) without clearly specifying what is meant by $d < L$, or, sometimes, postulating a periodic unit cell. Here we study this inequality for flow in porous media within a general framework of scale-dependent homogenization of random media (Ostoja-Starzewski, 2001) without any periodicity assumption, in the vein of Hill's (1963) definition of RVE.

In order to attain the said homogenization, two conditions in the homogeneous sense of Hill must be satisfied. Clearly, equations (2.1.1-2) show that Darcy's law shares the same mathematical formulation as conductivity problems. However, as stated by Torquato (2002), "*As in the trapping problem, there is no local*

constitutive relation in the flow problem." As is well known, the local governing equation of fluid in pore spaces is the Stokes equation.

At this point, let us briefly review prior work on permeability problems in porous media. Evidently, due to the complex, randomly structured nature of such media, deterministic solutions are not possible. Statistical methods are therefore often used for the determination of rigorous (upper/lower) bounds on the effective (RVE level) permeability. In the very early work done by Prager (1961), a variational principle of energy dissipation rate was applied and, with a proposed trial stress field, the upper bound was obtained. More rigorous bounds have been proposed by Berryman & Milton (1985) and a different trial stress with two point bounds was used. They were able to reduce the upper bound by a factor from 9/10 to 2/3. Another important approach has been invented and developed in (Rubinstein & Torquato, 1989). In their derivation of Darcy's Law from the Stokes equation, an energy-formed functional of permeability was formulated with the ensemble of the "tensor velocity field" and "vector pressure field". The variational principle was applied on this energy-formed functional, and both upper and lower bounds were obtained with properly selected of trail functions. While all the aforementioned works gave bounds on effective permeability, the size of RVE was only required to be much bigger than the microscale.

The response of that domain is therefore a function of (i) mesoscale δ, (ii) the boundary conditions, and (iii) the actual microstructure such as that shown in Fig. 1-2. Since the microstructure, in the ensemble sense, is random, the

mesoscale response is statistical, but tends to become deterministic as δ grows. It is this tendency in function of δ which is the focus of our study.

2.2 Mathematical Formulation

2.2.1 Variational Principles

In the general studies on property bounds, the variational principles usually provide the basic starting point (Prager, 1961; Huet, 1990; Jeulin & Ostoja-Starzewski, 2001; Torquato, 2002). Now, as mentioned before, Darcy's law (2.1.1-2) is not a local constitutive relation, since the slow flow in voids is governed by the Stokes equation:

$$\begin{cases} \mu \nabla^2 \vec{v} = \nabla p \\ \nabla \cdot \vec{v} = 0 \end{cases} \tag{2.2.1}$$

where $\vec{v}$ is the actual fluid velocity ($[m/s]$). In any chosen element dV of a porous medium the energy dissipation rate ϕ ($[J/m^3 \cdot s]$) in a fluid of viscosity μ is usually calculated as

$$\phi = \frac{1}{2\mu V} \int_{V_f} \sigma_{ij} \sigma_{ij} dV \tag{2.2.2}$$

where V_f is void region, σ_{ij} is a symmetric, zero-trace stress tensor ($[Pa]$), which can be obtained by solving the Stokes equation directly.

Let us now consider a trial stress field, $\tilde{\sigma}_{ij}$, satisfying

$$\tilde{\sigma}_{ij,j} = \tilde{p}_{,i} \quad \text{in} \quad V_f \tag{2.2.3}$$

where $\tilde{p}$ is a scalar function, a trial pressure field, such that

$$\tilde{p} = p^0 \text{ and } \tilde{\sigma}_{ij} = 0 \text{ in } \partial B \tag{2.2.4}$$

where ∂B is the surface of the domain B of the porous media. Prager (1961) and Berryman & Milton (1985) stated the variational principle for an element as follows

$$\tilde{\phi} = \frac{1}{2\mu V}\int_{V_f} \tilde{\sigma}_{ij}\tilde{\sigma}_{ij} dV \geq \overline{\frac{K_{ij}}{\mu} p_{,i} p_{,j}} \tag{2.2.5}$$

where $\tilde{\phi}$ is the trial dissipation rate calculated with the trial stress function. As we shall see in Section 2.2.3, this gives the upper bound on the effective permeability K_{ij} according to Prager (1961). The equality $\phi = \tilde{\phi}$ occurs only when $\tilde{\sigma}_{ij}$ is equal to the true stress, and this is equivalent to the law of energy conservation. This fact will be used in the subsequent numerical simulations.

On the other hand, the variational principle based on Darcy's law (2.1.2-3) can be expressed in term of the pressure gradient and the Darcy velocity. Hence, the energy dissipation rate in the porous domain can also be written as

$$\phi = \frac{1}{V}\int(-p_{,i} \cdot U_i) dV \tag{2.2.6}$$

Here we use another form of Darcy's law, in which the pressure gradient is a function of Darcy's velocity:

$$p_{,i} = -\mu R_{ij} \cdot U_j \quad \text{or} \quad \nabla p = -\mu \underline{R} \cdot \vec{U} \tag{2.2.7}$$

with R_{ij} ($\equiv \underline{R}$) being the resistance tensor of the porous medium.

For the effective tensors – that is, on the scale L where the separation of scales (1.2) holds - we have the following relation,

$$\underline{K}^{eff} \cdot \underline{R}^{eff} = \underline{I} \tag{2.2.8}$$

where $\underline{I}$ is the second-rank identity tensor. However, when the element scale is smaller than the RVE size, the foregoing relation is generally not true.

According to the preceding discussion, the energy dissipation can be expressed in two different quadratic forms,

$$\phi^P = \frac{1}{V}\int(\frac{K_{ij}}{\mu} p_{,i} p_{,j})dV \tag{2.2.9}$$

$$\phi^C = \frac{1}{V}\int(\mu R_{ij} U_i U_j)dV \tag{2.2.10}$$

If we look at Darcy's law (2.1.1-2), the following equation can easily be derived in the absence of sources and sinks inside the material domain:

$$\nabla \cdot (\underline{K} \cdot \nabla p) = 0 \tag{2.2.11}$$

Of course, when considering homogeneous and isotropic media, the foregoing equation becomes the Laplace equation.

Clearly, we see an analogy of the Ansatz of flow through random porous media to that of mechanics of solid random media (Jeulin & Ostoja-Starzewski, 2001). That is, the pair (pressure field, Darcy velocity) corresponds to the pair (strain, stress) in anti-plane elasticity, or the pair (temperature, heat flux) in heat conductivity. Then, ϕ^P is treated as the potential energy, while ϕ^C is the complementary energy.

Now, recall two variational principles in terms of potential and complementary energies, that is:

Principle 1: Among the admissible solutions for the pressure field in a porous medium domain, the true solution possesses the minimum potential energy.

Principle 2: Among the admissible solutions for the Darcy velocity field in a porous medium domain, the true solution possesses the minimum complementary energy.

As noted earlier, there is another energy formulation with associated variational principles (Torquato, 2002). However, as they do not involve mechanical boundary conditions, they will not be used in the present study.

2.2.2 Hill condition in porous media

When considering a mesoscale domain of the heterogeneous medium, the distribution of surface value will be used to evaluate the constitutive response. In the context of elasticity as defined by Huet (1990, 1995), this results in the so-called apparent properties. As a first step, the Hill condition must be satisfied. In an elastic heterogeneous material, that condition can be expressed as follows,

$$\overline{\sigma:\varepsilon} = \overline{\sigma}:\overline{\varepsilon} \Leftrightarrow \int_{\partial B} (t - \overline{\sigma}\cdot\vec{n})\cdot(u - \overline{\varepsilon}\cdot\vec{x})\, dS = 0 \qquad (2.2.12)$$

where $\vec{n}$ is the unit normal vector of a surface element dS, $\vec{x}$ is the coordinate of dS. Combining this with the average strain and stress theorems in elasticity, this ensures that the energetic definition is equivalent to the mechanical definition of

Hooke's law. Hence, the variational principles based on energy can be applied to evaluate the constitutive response of heterogeneous material in term of the boundary values.

Analogous to this, a similar theory must also be established in permeability of porous media. Thus, in a given porous medium domain V, the pressure gradient and the Darcy velocity can be expressed in the form of average values and fluctuations,

$$p_{,i} = \overline{p_{,i}} + p_{,i}' \tag{2.2.13}$$

$$U_i = \overline{U_i} + U_i' \tag{2.2.14}$$

The energy dissipation is calculated as,

$$-\phi = \overline{p_{,i}U_i} = \overline{p_{,i}}\,\overline{U_i} + \overline{p_{,i}'U_i'} \tag{2.2.15}$$

From the foregoing equation, it appears that, in general, the energy dissipation cannot be calculated from surface values, except only when $\overline{p_{,i}'U_i'} = 0$. By inspiration of Hill's condition in elasticity (Hill, 1963), the following derivation applies

$$\overline{p_{,i}'U_i'} = \overline{p_{,i}U_i} - \overline{p_{,i}}\,\overline{U_i} = \frac{1}{V}\int_V (p_{,i} - \overline{p_{,i}})(U_i - \overline{U_i})dV \tag{2.2.16}$$

Due to the continuity equation $U_{i,i} = 0$, we get

$$\overline{p_{,i}'U_i'} = \frac{1}{V}\iint_V \left[(p - \overline{p_{,j}}x_j)(U_i - \overline{U_i})\right]_{,i} dV \tag{2.2.17}$$

Applying the Green-Gauss theorem, we arrive at

$$\overline{p_{,i}'U_i'} = \frac{1}{V}\int_{\partial B}(p - \overline{p}_{,j}x_j)(U_i n_i - \overline{U}_i n_i)dS \tag{2.2.18}$$

Therefore, in order to satisfy $\overline{p_{,i}U_i} = \overline{p}_{,i}\overline{U}_i$, the term (2.2.18) must vanish. We conclude that the Hill condition for Darcy's law is

$$\overline{p_{,i}U_i} = \overline{p}_{,i}\overline{U}_i \Leftrightarrow \int_{\partial B}(p - \overline{p}_{,j}x_j)(U_i n_i - \overline{U}_i n_i)dS = 0 \tag{2..2.19}$$

To satisfy (2.2.19), there are three possible boundary conditions:

(i) $p = \overline{\nabla p}\cdot\vec{x}$, or $p = \overline{p}_{,i}x_i$ on ∂B (2.2.20)

(ii) $\vec{U}\cdot\vec{n} = \vec{U}_0\cdot\vec{n}$ or $U_i n_i = U_{0i}n_i$ on ∂B (2.2.21)

(iii) $(p - \overline{\nabla p}\cdot\vec{x})(\vec{U}\cdot\vec{n} - \vec{U}_0\cdot\vec{n}) = 0$ or $(p - \overline{p}_{,i}x_i)(U_i n_i - U_{0i}n) = 0$ on ∂B (2.2.22)

Following the terminology of thermomechanics of solid random media, (2.2.20) is called a *uniform Dirichlet* (or *essential*) boundary condition, (2.2.21) is called a *uniform Neumann* (or *natural*) boundary condition, while (2.2.22) is called a *uniform orthogonal-mixed* boundary condition. The Hill condition (2.2.19) ensures that the energy dissipation calculated from the surface values of the mesoscale element under either of these conditions is equal to the energy dissipation obtained from the volume integration over that element.

At this point we introduce apparent dissipation functionals on the mesoscale $\phi_\delta^P(\overline{\nabla p})$ and $\phi_\delta^C(\overline{U})$, which are homogeneous functions of degree 2 in the volume average pressure gradient $\overline{\nabla p}$ and the volume average Darcy velocity $\overline{U}$, respectively. Thus, we have (Ziegler, 1983)

$$\overline{U}_i = \frac{1}{2}\frac{\partial \phi^p}{\partial p_{,i}} \qquad \overline{p}_{,i} = \frac{1}{2}\frac{\partial \phi^C}{\partial U_i} \tag{2.2.23}$$

With this we have a full analogy between the Stokesian flow in porous media and the anti-plane elasticity in a matrix of finite stiffness, containing infinitely stiff inclusions.

Note that there is no body force considered in the above derivations. Also, the above derivations use the index notation for clarity. Further derivations will mostly use the symbolic notation for simplicity.

2.2.3 Scale dependent hierarchies of bounds

We take the porous medium as a set $B = \{B(\omega); \omega \in \Omega\}$ of realizations $B(\omega)$, defined over the sample space Ω. Thus, for an elementary event $\omega \in \Omega$, we have a realization $B(\omega)$, theoretically of infinite extent, from which we a cut out a mesoscale specimen $B_\delta(\omega)$, of finite size $L = \delta d$. That specimen is characterized by apparent (or mesoscale) permeability and resistance tensors according to

$$\vec{U} = \frac{\underline{\underline{K}}(\vec{x}, \omega)}{\mu} \cdot \nabla p \tag{2.2.24}$$

$$\nabla p = \mu \underline{\underline{R}}(\vec{x}, \omega) \cdot \vec{U} \tag{2.2.25}$$

We require the statistics of material properties to be statistically homogeneous and mean-ergodic. The latter property means that the spatial average equals the

ensemble average as the said in (1.3). Note, of course, that $\underline{K}^{app} = (\underline{R}^{app})^{-1}$ is not given by the above equality.

As a particular case, one may assume the statistics of microstructure to be isotropic, which would yield

$$\overline{\underline{K}(\omega)} = \langle \underline{K}(\vec{x}) \rangle = K\underline{I} \tag{2.2.26}$$

i.e. the isotropy of the effective response on the RVE level.

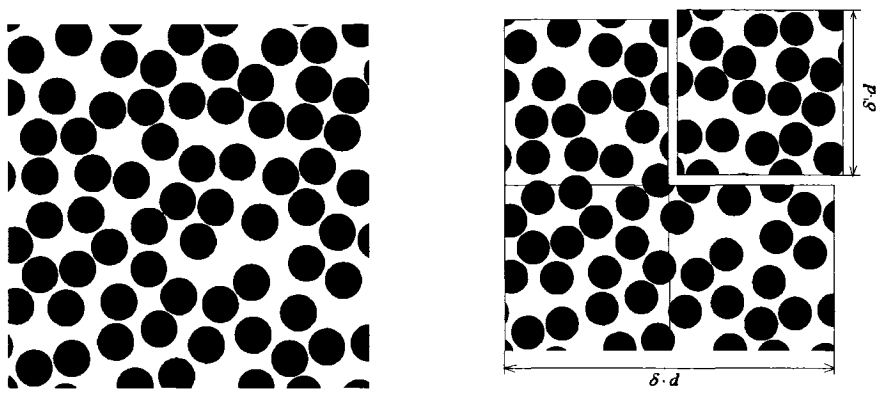

(a) (b)

Fig. 2-1. (a) A planar model of a random medium, formed from a non-overlapping distribution of circular disks; one deterministic configuration at a nominal porosity of 50% is shown. (b) Domain $B_\delta(\omega)$ and its partitioning into four subdomains $B^s_{\delta'}(\omega)$.

In the following, we partition a square-shaped $B_\delta(\omega)$ into 2^m subdomains $B^s_{\delta'}(\omega)$ (in 2-D, m = 2; in 3-D, m = 3), s = 1, 2, ... 2^m. Thus, each $B^s_{\delta'}(\omega)$ has the mesoscale $\delta' = \delta/2$. Clearly,

$$B_\delta(\omega) = \bigcup_{s=1}^{2^m} B^s_{\delta'}(\omega) \tag{2.2.27}$$

Henceforth, for simplicity, we work in 2-D as shown by Fig 2-1(b); the procedure is totally analogous in 3-D.

We now define two types of boundary conditions here — namely the "unrestricted" and "restricted" boundary conditions for $B_\delta(\omega)$ and all four $B^s_{\delta'}(\omega)$'s, respectively.

First, let us consider an "unrestricted" essential boundary condition: the prescribed pressure on the boundary of $B_\delta(\omega)$:

$$p = \overline{\nabla p} \cdot \vec{x} \qquad \text{on} \qquad \partial B_\delta(\omega) \tag{2.2.28}$$

In view of the Hill condition, the potential energy can be expressed as

$$\phi^P_\delta = \nabla p \cdot \frac{\underline{\underline{K}}^e}{\mu} \cdot \nabla p \,. \tag{2.2.29}$$

On the other hand, we can also set up a "restricted" essential boundary condition: the prescribed pressure on the boundary of all four $\partial B^s_{\delta'}(\omega)$ in (2.2.26):

$$p = \overline{\nabla p} \cdot \vec{x} \qquad \text{on} \qquad \partial B^s_{\delta'}(\omega); s = 1,...,4\,, \tag{2.2.30}$$

which, given the Hill condition, leads to

$$\phi^P_\delta = \nabla p \cdot \frac{\underline{\underline{K}}^{er}}{\mu} \cdot \nabla p \tag{2.2.31}$$

where $\underline{K}^{er}$ is a tensor different from $\underline{K}^{e}$ in (2.2.28), where r denotes the restriction.

We now observe that the solution under the restricted boundary condition (2.2.29) on all four subdomains $B^{s}_{\delta'}(\omega)$ is an admissible solution with respect to the unrestricted boundary condition on $B_{\delta}(\omega)$, but not *vice versa*. Thus, in view of the minimum potential energy principle, we have the inequality: $\phi_{\delta}{}^{P} \leq \sum_{s=1}^{4} \phi^{sr}_{\delta'}{}^{P}$. Henceforth, given (2.28), this inequality relationship becomes

$$V_{\delta} \nabla p \cdot \frac{\underline{K}_{\delta}{}^{e}}{\mu} \cdot \nabla p \leq \sum_{s=1}^{4} V^{s}_{\delta'} \nabla p \cdot \frac{\underline{K}_{\delta'}{}^{es}}{\mu} \cdot \nabla p \tag{2.2.32}$$

Note that $V_{\delta} = 4V_{\delta'}$ here. Consequently, the following relationship can be obtained upon taking the ensemble average over the space Ω

$$\left\langle \underline{K}_{\delta}{}^{e} \right\rangle \leq \left\langle \underline{K}_{\delta'}{}^{es} \right\rangle . \qquad \forall \delta' = \delta/2 \tag{2.2.33}$$

Note here the inequality is taken as stated after hierarchy (1.5). By induction, (2.2.33) leads to a scale-dependent hierarchy (upper bound) of the permeability of porous media flow

$$\underline{K}^{eff} \leq \cdots \leq \left\langle \underline{K}_{4\delta}{}^{e} \right\rangle \leq \left\langle \underline{K}_{2\delta}{}^{e} \right\rangle \leq \left\langle \underline{K}_{\delta}{}^{e} \right\rangle \leq \cdots \leq \left\langle \underline{K}_{1}{}^{e} \right\rangle \tag{2.2.34}$$

Note that $\left\langle \underline{K}_{1}{}^{e} \right\rangle$ pertains to the smallest scale where Darcy's law still applies; by analogy to elasticity of random media, that tensor may be called a Voigt bound.

Now, let us consider an "unrestricted" natural boundary condition: the prescribed velocity on the boundary of $B_\delta(\omega)$:

$$\vec{U}\cdot\vec{n}=\vec{U}_0\cdot\vec{n} \quad \text{on} \qquad \partial B_\delta(\omega). \tag{2.2.35}$$

and a "restricted" natural boundary condition: the prescribed velocity on the boundary of all four $\partial B^s_{\delta'}(\omega)$ in (2.2.26):

$$\vec{U}\cdot\vec{n}=\vec{U}_0\cdot\vec{n} \quad \text{on} \qquad \partial B^s_{\delta'}(\omega); s=1,...,4 \tag{2.2.36}$$

We now consider the energy dissipation rate via the analogy to complementary energy under (2.2.34) and (2.2.35), respectively. Note that the Hill condition is applicable in both cases. Then, in view of the minimum complementary energy principle (of Section 2.2.1), the solution under the restricted boundary condition (2.2.35) is admissible with respect to the unrestricted boundary condition (2.2.34), but not vice versa. Hence,

$$V_\delta\vec{U}_0\cdot\mu\underline{R}_\delta{}^n\cdot\vec{U}_0\le\sum_{s=1}^{4}V^s_{\delta'}\vec{U}_0\cdot\mu\underline{R}^{s}_{\delta'}{}^{n}\cdot\vec{U}_0 \tag{2.2.37}$$

As before, upon taking the ensemble average over the space Ω, we arrive at the inequality for the resistance tensor on two mesoscales, δ and δ',

$$\left\langle\underline{R}_\delta{}^n\right\rangle\le\left\langle\underline{R}_{\delta'}{}^{ns}\right\rangle \qquad \forall\delta'=\delta/2 \tag{2.2.38}$$

Clearly, this indicates the upper bound character of resistance tensors with respect to $\underline{R}^{eff}=(\underline{K}^{eff})^{-1}$. Since δ is arbitrary, we have a scale-dependent hierarchy (of lower bounds) of the inverse of resistance tensor of porous media flow

$$\underline{R}^{eff\,-1} \geq \cdots \geq \left\langle \underline{R}_{4\delta}{}^{n} \right\rangle^{-1} \geq \left\langle \underline{R}_{2\delta}{}^{n} \right\rangle^{-1} \geq \left\langle \underline{R}_{\delta}{}^{n} \right\rangle^{-1} \geq \cdots \geq \left\langle \underline{R}_{1}{}^{n} \right\rangle^{-1} \tag{2.2.39}$$

The hierarchies (2.2.31) and (2.2.36) can be combined into a single, two-sided hierarchy:

$$\left\langle \underline{K}_{\delta}{}^{es} \right\rangle \geq \left\langle \underline{K}_{2\delta}{}^{e} \right\rangle \geq \cdots \geq \underline{K}^{eff} = (\underline{R}^{eff})^{-1} \geq \cdots \geq \left\langle \underline{R}_{2\delta}{}^{n} \right\rangle^{-1} \geq \left\langle \underline{R}_{\delta}{}^{n} \right\rangle^{-1} \tag{2.2.40}$$

This relation states that, for random heterogeneous porous media which are statistically homogeneous and egordic,

(i) the effective permeability tensor is bounded from above by the permeability tensor obtained under the essential boundary condition, and from below by the permeability tensor obtained under the natural boundary condition;

(ii) the hierarchy (2.2.40) shows the scale dependence of apparent permeability tensors under essential or natural boundary condition, which with the increasing mesoscale δ tend to converge towards the effective permeability.

2.3. The RVE size via computational fluid mechanics

2.3.1 Direct simulation

The foregoing discussion also indicates a procedure to quantitatively homogenize the heterogeneous medium and determine the RVE size. In the following, we conduct numerical simulations to demonstrate the converging

tendency of hierarchy (2.2.40) quantitatively. Starting from the energy conservation law in (2.2.5), we solve Stokes' equation (2.2.1) numerically in the void of a random model for a given boundary condition, either essential or natural. In order to deal with the geometric complexity of random porous media, we employ a Control Volume Finite Difference Method (CVFDM), and to avoid the enhancement of incompressibility by Stokes flow which causes an unrealistic oscillation of the pressure field in computation, a so-called Semi-Implicit Method for Pressure-Linked Equations Revised (SIMPLER) with collocated equal-order discretization technique is used (Chung, 2000; Patankar, 1980).

The porous media model investigated in the present research is a two-dimensional flow past a bed of round disks randomly distributed by a planar Poisson point process with inhibition (Fig 2-1a). The latter condition means that no two disks may touch. In fact, in order to avoid the narrow-neck effects in fluid field, the minimum distance between disk centers is set at 1.1 diameter of the disk. Such effects may be introduced as an extension of our model in future work.

We set up boundary conditions for Darcy's law. First, for the essential boundary condition with $\overline{\nabla p}$ prescribed by (2.2.20) for a mesoscale specimen at a given δ, we must also pose a proper boundary condition for the Stokes flow in the void region. Beside the pressure distribution (2.2.20), and according to (2.2.3) and (2.2.4), we set $v_{1,2} = 0$ on the top and bottom of the element, and $v_{2,1} = 0$ on the left and right side of the element for the direct numerical simulation of the void region. This leads to a calculation of the mesoscale permeability tensor K_{ij}.

On the other hand, for the natural boundary condition, given $\vec{U}$ in (2.2.21), also according to (2.2.3) and (2.2.4), we set $v_2 = 0$ on the top and bottom boundaries of the element. This allows us to calculate the mesoscale resistance tensor R_{ij}.

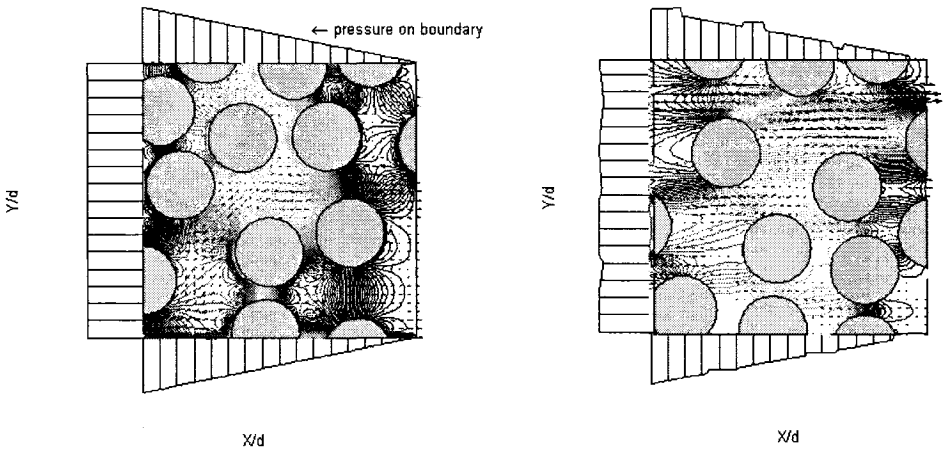

(a) Dirichlet b.c. ($\delta = 4$) (b) Neumann b.c. ($\delta = 4$)

Fig. 2.2. Pressure field in a realization of the random porous medium under two different boundary conditions (b.c.).

Figure 2-2 illustrates the comparison between both kinds of boundary conditions. We can clearly see in (b) that the pressure distributes non-linearly on side boundaries in order to maintain the flow within the top and bottom boundary according to the requirement of Neumann boundary condition. Nevertheless, for a sufficiently large mesoscale, the fluctuation of pressure becomes so negligible that the results of the natural boundary value problem begin to coincide with those of the essential boundary value problem (except for the obvious non-uniqueness of the natural problem). This is the RVE limit we want to assess.

2.3.2 Numerical results and discussion

To assess the hierarchy (2.2.40), we proceed in the following steps:

(a) choose a specific mesoscale δ and a nominal porosity;

(b) generate a mesoscale realization $B_\delta(\omega)$ of the disordered medium as described in Section 3.1;

(c) separately solve the essential and natural boundary value problems for each $B_\delta(\omega)$, and store the apparent permeability and resistance tensors: $\mathbf{K}_\delta(\omega)$ and $\mathbf{R}_\delta(\omega)$;

(d) proceed from (a) to (c) in a Monte Carlo sense over the sample space Ω to generate an ensemble of results at a fixed mesoscale δ: $\{\mathbf{K}_\delta(\omega); \omega \in \Omega\}$ and $\{\mathbf{R}_\delta(\omega); \omega \in \Omega\}$;

(e) change the mesoscale and repeat steps (a) to (d) to find the first moments $\left\langle \mathbf{K}_\delta^D \right\rangle$ and $\left\langle \mathbf{R}_\delta^N \right\rangle$;

(f) change the nominal porosity and repeat steps (a) to (e).

In this procedure, we use $\delta = 2$, 4, 8, 16, 32, 64, and 80, and nominal porosities 50%, 60%, 70%, and 80%.

Figure 2-3 displays the simulation results of the random medium at 60% porosity in terms of the ensemble average half-traces of the permeability and resistance tensors. The bounding character of these tensors and their convergence to the RVE (effective medium) with the increasing mesoscale are clearly seen. In

fact, at δ = 80, the ensemble averages of both tensors are approximately equal within 0.4%.

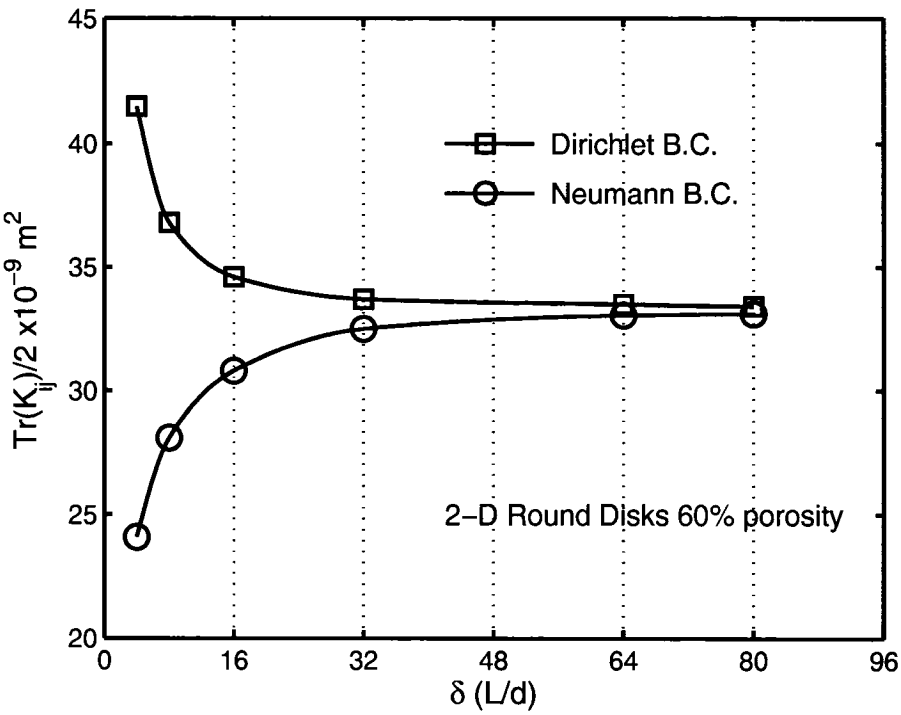

Fig. 2-3. Effect of increasing window scale on the convergence of the hierarchy (2.2.40) of mesoscale bounds for the numerical model.

Another viewpoint of that convergence to RVE may be offered in terms of the departure of one half of the ensemble averaged scalar product of $\mathbf{K}_\delta^D(\omega)$ and $\mathbf{R}_\delta^N(\omega)$ from unity, for we must have at $\delta = \infty$

$$\frac{1}{2}\mathbf{K}^{eff} \cdot \mathbf{R}^{eff} = 1 \tag{2.3.1}$$

The statistical isotropy of the underlying Poisson point field with exclusion dictates the isotropy of not only effective (RVE level) properties but also the isotropy of $\left\langle \mathbf{K}_{\delta}^{D} \right\rangle$ and $\left\langle \mathbf{K}_{\delta}^{N} \right\rangle$.

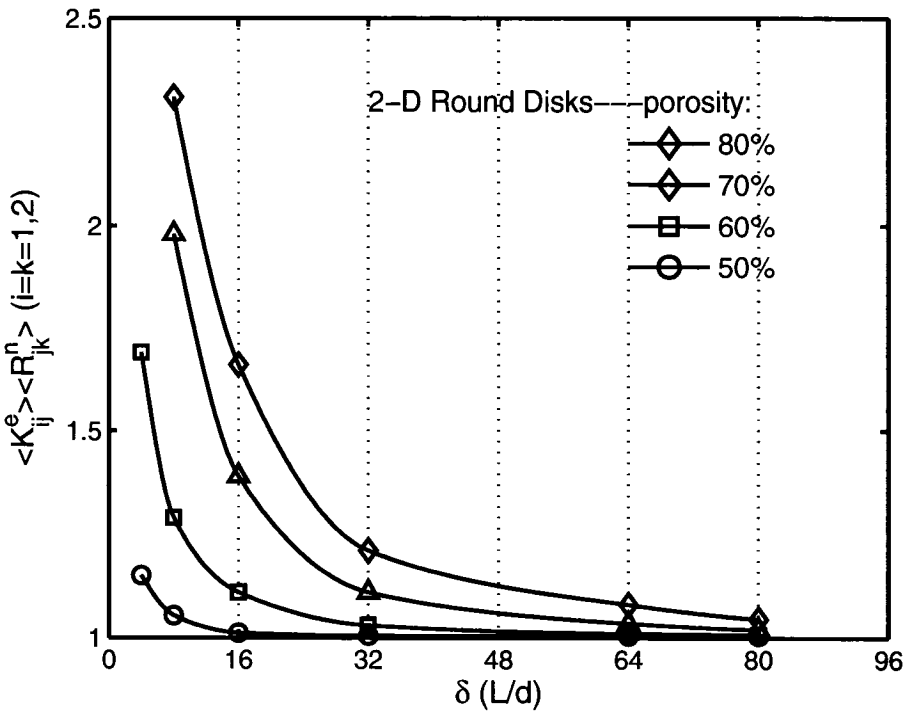

Fig. 2-4. Effect of increasing window scale on the convergence of (2.40) in function of mesoscale δ for the numerical model.

Thus, we can work with

$$D = K^{D}_{\delta 1j} R^{N}_{\delta 1j} - 1 \tag{2.3.2}$$

to characterize the above mentioned departure from the RVE properties; here $1j$ are the indices of particular components of the $\underline{K}_{\delta}^{D}$ and $\underline{R}_{\delta}^{N}$ tensors, and D is departure from unit. The said departure is shown in Fig. 2.4, both for the preceding case of porosity, as well as for the entire range: 50% through 80%.

Clearly, the scaling effect of permeability in porous media depends more strongly on the size of micro-channels than on the disk diameter d itself. The rate of convergence to RVE decreases with the porosity increasing. For example, at δ = 32, the RVE size can be considered to be attained at porosity 50%. However, for a higher porosity, say 80%, the RVE size is still not achieved even at $\delta = 80$.

Of course, the rate of convergence to RVE also depends on the acceptable error. Therefore, in Fig. 2.5, we show D with respect to the scale change and porosities. We can see that, for a 10% error, in the medium with 80% porosity, the RVE can be reached at the mesoscale $\delta = 56$. However, for a 1% error, it cannot be reached even at $\delta \cong 100$.

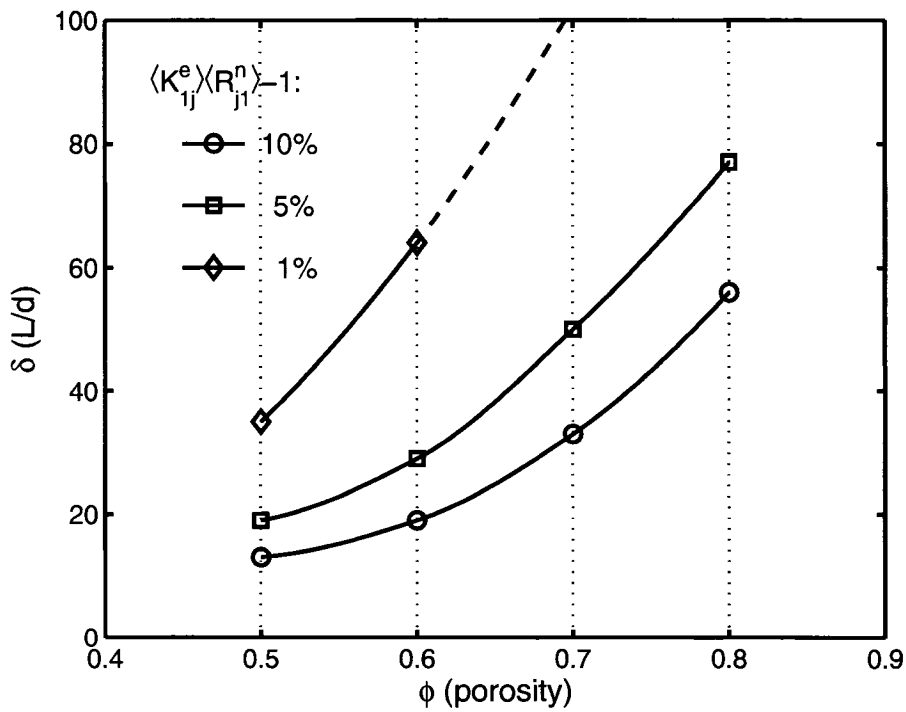

Fig. 2.5. The effects of porosity and mesoscale on the departure of permeability from that of the effective medium (RVE level).

As a final issue, we assess the rate of convergence to the isotropic behavior. That property is measured using the second invariant of either $K_\delta(\omega)$ or $R_\delta(\omega)$, i.e. the radius of the Mohr circle of the second rank tensor

$$r = \sqrt{\left(\frac{K_{11} - K_{22}}{2}\right)^2 + K_{12}^2} \tag{2.3.3}$$

Also the variance of r converges to zero as well. Figure 2.6 shows the coefficient of variation of r (i.e. its standard deviation divided by the mean) in function of the mesoscale (r has the same unit as K). We see that the variance converges to zero faster than the ensemble average in the present study.

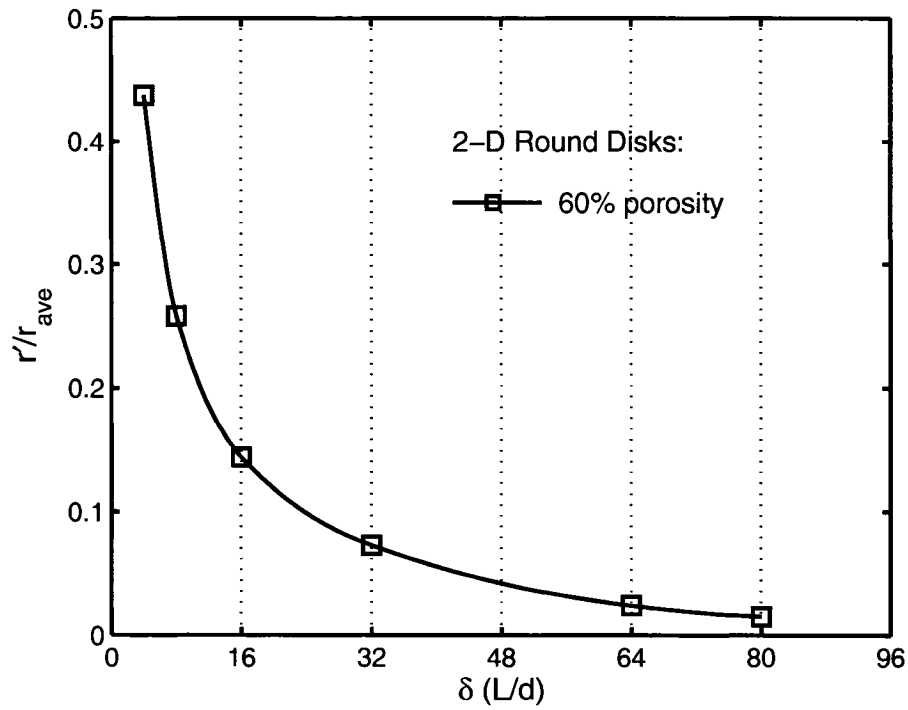

Fig. 2.6. The standard deviation of r over the ensemble average of r for the 60% porosity medium.

2.4. Closure

We summarize this study as follows:

(a) We set up the mathematical basis for finding effective permeability and RVE size for porous media with spatially homogeneous and ergodic statistics. By analogy to the existing methodology in thermomechanics of solid random media, we first formulate a Hill-Mandel condition for the Darcy flow velocity and pressure gradient fields. This dictates uniform Neumann and Dirichlet boundary conditions, which, with the help of the minimum potential and complementary energy principles for the Stokes flow, lead to scale dependent hierarchies on effective (RVE level) permeability.

(b) The scale-dependent hierarchy of mesoscale bounds on the effective (RVE level) permeability tensor is derived: the ensemble average of the permeability tensor is bounded from above by Dirichlet boundary value problems, and from below by Neumann boundary value problems. The upper and lower bounds converge towards the RVE response with the window scale increasing.

(c) The hierarchy of bounds is computed for a range of volume fractions of random media made up of planar disks, where the disk centers are generated by a planar Poisson process with inhibition. Overall, it turns out that the higher is the density of

random disks – or, equivalently, the narrower are the micro-channels in the system – the smaller is the size of the RVE pertaining to the Darcy law. In particular, the condition $d << L$ in the separation of scales (1.1) is not always necessary, and it is possible that the RVE is attained at $d < L$.

This study sets the stage for computation of the RVE size in permeability of 3-D microstructures, as well as for extensions to poroelasticity, where the fluid flows in an elastic microstructure. This will be discussed further in Chapter 4.

Chapter 3

On Scaling from Statistical to Representative Volume Element in Thermoelasticity of Random Materials[*]

3.1. Introduction

The thermal expansion phenomenon reflects a coupling between mechanical and thermal fields. The 'separation of scales' as in (1.2) is also an important concept for RVE of liner thermoelasticity. In the case of spatial disorder having no microstructural periodicity, the RVE concept implies that there must be a scale (much) larger than the microscale (e.g., single heterogeneity size) to ensure a homogenization limit in the sense of Hill (1963) on which all of the deterministic continuum mechanics/physics hinges.

In general, the size of the RVE depends on several characteristics of microstructures, principal of which are: random microgeometries, mismatch in mechanical properties of individual phases, and the actual physics involved. The present research extends the similar methodology in chapter 2 to mesoscale bounds in a coupled field problem: thermal expansion coefficients, effective stiffness, and specific heat of linear thermoelastic microstructures.

Our analysis is based on variational principles of thermoelasticity, combined with the assumption of statistical homogeneity and ergodicity of the random

---

[*] Most of this chapter has been published as an article in Networks and Heterogeneous Media Vol. 1, No. 2, 2006

medium, without any spatial periodicity assumptions. On that basis we derive hierarchies of scale-dependent tensors, bounding the RVE responses from above (and below) under uniform essential (respectively, uniform natural) boundary conditions. Using computational mechanics, we then quantitatively demonstrate the trend of these hierarchies to converge toward the RVE responses on the example of a two-phase random matrix-inclusion composite in two dimensions (2-D).

3.2. Theoretical Fundamentals

3.2.1 Random microstructure

Again, we take the random material to be a set $B=\{B(\omega);\omega\in\Omega\}$ of realizations $B(\omega)$, defined over the sample space Ω. Thus, for an elementary event $\omega\in\Omega$, we have a realization $B(\omega)$, theoretically of infinite extent. From $B(\omega)$ we isolate an arbitrary mesoscale specimen $B_\delta(\omega)$, of finite size $L=\delta d$, Fig. 2-1(a). Ideally, $\delta\to\infty$ leads to homogeneous properties of heterogeneous materials. However, depending on the actual microstructural parameters, δ can be anything from a moderate to a very large number such that RVE is achieved within a required accuracy. It is the assessment of such a trend that is of interest to us here.

We require all the statistics of material properties to be spatially homogeneous and mean-ergodic. While the first property implies the invariance of all n-point distributions with respect to arbitrary shifts in spatial domain, the latter property

means that the spatial average for any fixed realization $B(\omega)$ equals the ensemble average at any fixed point in the material domain, see in (1.3). More rigorous statements of the required ergodic properties of the material were given by Sab (1992). We assume the composite to be made of perfectly bonded phases, i.e. there are no displacement discontinuities.

3.2.2 Constitutive laws in thermoelastic problems

Locally (i.e. in each phase), the thermoelastic constitutive response is written as either

$$\varepsilon_{ij} = S_{ijkl}(\omega, x)\sigma_{kl} + \alpha_{ij}(\omega, x)\theta \tag{3.2.3}$$

or

$$\sigma_{ij} = C_{ijkl}(\omega, x)\varepsilon_{kl} + \Gamma_{ij}(\omega, x)\theta \tag{3.2.4}$$

where the thermal stress coefficient $\Gamma_{ij}([Pa/K])$ is linked to the thermal expansion coefficient $\alpha_{kl}([1/K])$ by

$$\Gamma_{ij}(\omega, x) = -C_{ijkl}(\omega, x)\alpha_{kl}(\omega, x) \tag{3.2.5}$$

Clearly, the constitutive law in thermoelasticity involves three aspects:

(i) Linear elastic relation between stress and strain

$$\sigma_{ij} = C_{ijkl}(\omega, x)\varepsilon_{kl} \text{ and } \varepsilon_{ij} = S_{ijkl}(\omega, x)\sigma_{kl} \tag{3.2.6}$$

where for homogeneous or effective we can have

$$C^*_{ijkl} = S^{*-1}_{ijkl}. \tag{3.2.7}$$

Hereinafter, the superscript * indicates an effective property of a homogenized material (i.e. at the RVE level).

(ii) For thermal expansion in terms of the temperature change, the relations between the thermal strain/stress and temperature are as follows,

$$\varepsilon_{ij} = \alpha^*_{ij}\theta \text{ and } \sigma_{ij} = \Gamma^*_{ij}\theta, \tag{3.2.8}$$

where α^*_{ij} and Γ^*_{ij} are thermal expansion and stress coefficients respectively. Clearly, for a homogenized medium, the following relation holds (Christensen 1979)

$$\Gamma^*_{ij} = -C^*_{ijkl}\alpha^*_{kl}. \tag{3.2.9}$$

(iii) Considering the heat (thermal) energy in terms of the temperature change $\theta = \Delta T = T - T_0$ ($[K]$), we either have the specific heat c_v ($[J/m^3 \cdot K]$) at constant volume, or specific heat c_p ($[J/m^3 \cdot K]$)at constant pressure. The two are related by

$$c^*_p - c^*_v = T_0 C^*_{ijkl}\alpha^*_{ij}\alpha^*_{kl}. \tag{3.2.10}$$

The equations (3.2.7), (3.2.9) and (3.2.10) hold at homogeneous phase. However, when we go to the mesoscale $\delta > 1$, these reciprocities are no longer assured, When we reach a medium homogenized at the level of of RVE ($\delta \to \infty$), the reciprocities are recovered. So as the projective stated for this study, what

mesoscale δ is needed to actually approximate the RVE level with a good accuracy?

3.2.3 Energetic formulations for heterogeneous materials

In mechanics of elastic and inelastic heterogeneous materials, energetic approaches are widely used, especially when setting up variational principles used to bound the effective properties. Energy concepts appear also in the so-called Hill (or Hill-Mandel) condition (Hill, 1963), which guarantees the equivalence of the mechanical and energetic approaches when determining the constitutive response, both at the macroscale and mesoscale levels. Thus, if stress and strain tensors are decomposed into their spatial average and fluctuation parts ($\sigma_{ij} = \overline{\sigma}_{ij} + \sigma'_{ij}$, $\varepsilon_{ij} = \overline{\varepsilon}_{ij} + \varepsilon'_{ij}$), the Hill condition states in (2.2.12). The detailed derivation on Hill condition is shown in Appendix A. This shows that when the boundary conditions satisfy the right hand side in (2.2.12) which leads to three types of boundary conditions in (A-4~6), the average of the product of the strain tensor and the stress tensor is equal to the product of averages. In other words, $\int_V \sigma'_{ij} : \varepsilon'_{ij} dv = 0$ must hold.

With reference to fundamentals of thermoelasticity theory, the Helmholtz free energy density per unit volume is

$$\sigma_{ij} = \left(\frac{\partial A}{\partial \varepsilon_{ij}} \right)_T \tag{3.2.12}$$

$$S = -\left(\frac{\partial A}{\partial T} \right)_{\varepsilon_{ij}} \tag{3.2.13}$$

where S is entropy ($[J/K]$), A is Helmholtz free energy ($[J/m^3]$) . When considering a small temperature change θ, the Helmholtz free energy is (Christensen 1979),

$$A=\frac{1}{2}C_{ijkl}\varepsilon_{ij}\varepsilon_{kl}+\Gamma_{ij}\varepsilon_{ij}\theta-\frac{1}{2}c_v\frac{\theta^2}{T_0} \tag{3.2.14}$$

where c_v is the specific heat under constant volume.

According to the Legendre transformation, the potential energy $U^P([J/m^3])$ is defined as,

$$U^P=\frac{1}{V}(\int_V Adv-\int_V F_i u_i dv-\int_{S_\sigma} t_i u_i dS) \tag{3.2.15}$$

where S_t is the part of boundary with traction prescribed on it, while F_i is the body force.

On the other hand, the Gibbs free energy G ($[J/m^3]$) is

$$G=-\frac{1}{2}S_{ijkl}\sigma_{ij}\sigma_{kl}-\alpha_{ij}\sigma_{ij}\theta-\frac{1}{2}c_p\frac{\theta^2}{T_0} \tag{3.2.16}$$

where c_p is the specific heat under constant traction, and the constitutive laws are

$$\varepsilon_{ij}=-\left(\frac{\partial G}{\partial \sigma_{ij}}\right)_{T_0} \tag{3.2.17}$$

$$S=-\left(\frac{\partial G}{\partial T}\right)_{\sigma_{ij}} \tag{3.2.18}$$

Again by the Legendre transformation, the complementary energy is defined as

$$U^C = -\frac{1}{V}\left(\int_V G dv + \int_{S_u} t_i u_i ds\right) \tag{3.2.19}$$

where S_u is the part of boundary with displacement prescribed on it.

The homogenized heterogeneous materials should take the energy formulation for homogeneous material. The energy formula same as homogeneous material is always applied to heterogeneous material without proof. It is only based on the assumption of RVE. However, when the size of RVE is not reached, the formula for the mesoscale element needs to be clarified in order to study scale effects in material properties.

First let us consider a material domain under a prescribed displacement condition $u_i(\vec{x}) = \varepsilon_{ij}^0 x_j$ on ∂B_δ and in the absence of body forces. In the special case of a homogeneous material, the potential energy is

$$U^P = \frac{1}{2} C_{ijkl} \varepsilon_{ij} \varepsilon_{kl} + \Gamma_{ij} \varepsilon_{ij} \theta - \frac{1}{2} c_v \frac{\theta^2}{T_0} \tag{3.2.20}$$

Following the usual approach in thermoelasticity, the total strain ε_{ij} can be considered as a superposition of two parts

$$\varepsilon_{ij} = e_{ij} + \varepsilon_{ij}^{th} \tag{3.2.21}$$

where e_{ij} is the elastic strain and ε_{ij}^{th} is the thermal strain (inelastic strain).

In the presence of a heterogeneous microstructure of the material domain (such as that in Fig. 2-1(a)), the potential energy is a result of integration over all the individual phases

$$U^P = \frac{1}{V}[\int_V (\frac{1}{2} C_{ijkl}\varepsilon_{ij}\varepsilon_{kl} + \Gamma_{ij}\varepsilon_{ij}\theta - \frac{1}{2}c_v\frac{\theta^2}{T_0})dV - \int_{S_t} t_i u_i dS] \tag{3.2.22}$$

The second term on the right hand side in the equation (3.2.22) is zero since S_t is an empty set. Upon substituting (3.2.21) into (3.2.22), we obtain

$$U^P = \frac{1}{V}\int_V [\frac{1}{2} C_{ijkl}(e_{ij} + \varepsilon_{ij}^{th})\varepsilon_{kl} + \Gamma_{ij}(e_{ij} + \varepsilon_{ij}^{th})\theta - \frac{1}{2}c_v\frac{\theta^2}{T_0}]dV \tag{3.2.23}$$

Substituting Hooke's law into (3.3.23) ($\sigma_{kl} = C_{klij}e_{ij}$, here e_{ij} is elastic part in (3.2.21)) and the classical relation $\Gamma_{kl} = -C_{klij}\alpha_{ij}$, (3.2.23) transforms to the following

$$U^P = \frac{1}{V}\int_V [\frac{1}{2} C_{ijkl}e_{ij}\varepsilon_{kl} + \frac{1}{2} C_{ijkl}\varepsilon_{ij}^{th}\varepsilon_{kl} + \Gamma_{ij}(e_{ij} + \varepsilon_{ij}^{th})\theta - \frac{1}{2}c_v\frac{\theta^2}{T_0}]dV$$

$$= \frac{1}{V}\int_V [\frac{1}{2} C_{ijkl}e_{ij}\varepsilon_{kl} + \frac{1}{2} C_{ijkl}\alpha_{ij}\theta\varepsilon_{kl} + \Gamma_{ij}(e_{ij} + \varepsilon_{ij}^{th})\theta - \frac{1}{2}c_v\frac{\theta^2}{T_0}]dV$$

$$= \frac{1}{V}\int_V [\frac{1}{2} C_{ijkl}e_{ij}\varepsilon_{kl} - \frac{1}{2}\Gamma\theta\varepsilon_{kl} + \Gamma_{ij}(e_{ij} + \varepsilon_{ij}^{th})\theta - \frac{1}{2}c_v\frac{\theta^2}{T_0}]dV$$

$$= \frac{1}{V}\int_\Omega [\frac{1}{2}\sigma_{ij}\varepsilon_{ij} + \frac{1}{2}\Gamma_{ij}\varepsilon_{ij}\theta - \frac{1}{2}c_v\frac{\theta^2}{T_0}]dV \tag{3.2.24}$$

Next, take Γ_{ij} at every point to be the sum of the volume average

$$\overline{\Gamma}_{ij} = \frac{1}{V}\int_V \Gamma_{ij} dv \tag{3.2.25}$$

and a local fluctuation, that is $\Gamma_{ij} = \overline{\Gamma}_{ij} + \Gamma_{ij}^{'}$. We can decompose the strain in the same fashion: $\varepsilon_{ij} = \overline{\varepsilon}_{ij} + \varepsilon_{ij}^{'}$. Now, in view of the Hill condition (2.2.12) in linear elasticity and the fact that the temperature change θ is spatially uniform, from (3.2.24) we obtain

$$U^P = \frac{1}{2}\overline{\sigma}_{ij}\overline{\varepsilon}_{ij} + \frac{1}{2}\overline{\Gamma}_{ij}\overline{\varepsilon}_{ij}\theta + \frac{1}{V}\int_V (\frac{1}{2}\Gamma_{ij}^{'}\varepsilon_{ij}^{'}\theta) dV + \frac{1}{2}\overline{c}_v\frac{\theta^2}{T_0} \tag{3.2.26}$$

We can further consider the fluctuation of strain $\varepsilon_{ij}^{'}$ to consist of two parts

$$\varepsilon_{ij}^{'} = e_{ij}^{'} + \varepsilon_{ij}^{th'} \tag{3.2.27}$$

Moreover, we note that $e_{ij}^{'}$ is a function of displacement boundary condition (i.e. the applied strain ε_{kl}^0) and $\varepsilon_{ij}^{th'}$ is a function of temperature, so that we can write

$$e_{ij}^{'}(x) = D_{ijkl}(x)\varepsilon_{kl}^0 \tag{3.2.28}$$

$$\varepsilon_{ij}^{th'}(x) = E_{ij}(x)\theta \tag{3.2.29}$$

Here we introduce the tensor $D_{ijkl}(x)$ that relates the applied strain ε_{kl}^0 to the elastic strain fluctuation $e_{ij}^{'}$, and the tensor $E_{ij}(x)$ that relates the temperature change to the thermal strain fluctuation. Substituting (3.2.27-29) into (3.3.26), results in

$$U_\delta^P(\varepsilon_{ij}^0, \theta, \omega) = \frac{1}{2}\overline{\sigma}_{ij}\varepsilon_{ij}^0 + \frac{1}{2}(\overline{\Gamma}_{ij} + \frac{1}{V}\int_V D_{ijkl}\Gamma_{kl}^{'} dV)\varepsilon_{ij}^0\theta - \frac{1}{2}(\overline{c}_v - \frac{T_0}{V}\int_V \Gamma_{ij}^{'}E_{ij} dV)\frac{\theta^2}{T_0} \tag{2.30}$$

Here we write explicitly that U^P is a functional of the applied strain ε_{ij}^0, the temperature increment θ, the actual realization of the microstructure $B(\omega)$, and the mesoscale δ. The foregoing derivation indicates that, for heterogeneous materials, the potential energy can be expressed in the same type of a bilinear form as that for the homogeneous material (3.2.20), that is

$$U_\delta^P(\varepsilon_{ij}^0,\theta,\omega)=\frac{1}{2}C_{ijkl,\delta}(\omega)\varepsilon_{ij}^0\varepsilon_{kl}^0+\Gamma_{ij\,\delta}(\omega)\varepsilon_{ij}^0\theta-\frac{1}{2}c_{v,\delta}(\omega)\frac{\theta^2}{T_0} \tag{3.2.31}$$

providing that the mesoscale properties are identified as follows

$$\Gamma_{ij,\delta}(\omega)=\overline{\Gamma}_{ij}+\frac{1}{V}\int D_{ijkl}\Gamma_{kl}^{'}dV\,,\ c_{v,\delta}(\omega)=\overline{c}_v-\frac{T_0}{V}\int_V E_{ij}\Gamma_{ij}^{'}dV \tag{3.2.32}$$

In the case of the traction controlled boundary condition $t_i(\vec{x})=\sigma_{ij}^0 n_j$ on ∂B_δ, the complementary energy density for the homogeneous material is

$$U^C=\frac{1}{2}S_{ijkl}\sigma_{ij}\sigma_{kl}+\alpha_{ij}\sigma_{ij}\theta+\frac{1}{2}c_p\frac{\theta^2}{T_0} \tag{3.2.33}$$

Turning to the case of a heterogeneous microstructure on mesoscale, we can proceed in an analogous way as above, by noting that:

(i) The Hill condition must be satisfied.

(ii) The total stress ε_{ij} consists of the elastic and thermal parts, recall (3.2.19).

(iii) S_u is an empty set.

(iv) The thermal expansion coefficient α_{ij} as well as the local stress can be decomposed into the volume average part and the fluctuation part,

$$\alpha_{ij} = \overline{\alpha}_{ij} + \alpha_{ij}^{'} \text{ and } \sigma_{ij} = \overline{\sigma}_{ij} + \sigma_{ij}^{'} \tag{3.2.34}$$

(v) The stress fluctuation part $\sigma_{ij}^{'}$ can be considered to be made up of two parts: one caused by the applied traction on the domain boundary, and the other by the temperature change θ, the same fashion as in (A.8), i.e.

$$\sigma_{ij}^{'} = \sigma_{ij}^{e'} + \sigma_{ij}^{th'} \tag{3.2.35}$$

(vi) A transformation is formed to set up the relations between $\sigma_{ij}^{e'}$ and $\sigma_{ij}^{th'}$ in terms of the traction prescribed on the boundary σ_{ij}^{0} and the temperature change θ, i.e.

$$\sigma_{ij}^{e'}(x) = F_{ijkl}(x)\sigma_{kl}^{0} \tag{3.2.36}$$

$$\sigma_{ij}^{th'}(x) = H_{ij}(x)\theta \tag{3.2.37}$$

This then leads to the following expression for the complementary energy on mesoscale

$$U_{\delta}^{C}(\sigma_{ij}^{0},\theta,\omega) = \frac{1}{2}\sigma_{ij}^{0}\overline{\varepsilon}_{ij} + \frac{1}{2}(\overline{\alpha}_{ij} + \frac{1}{V}\int_{V} F_{ijkl}\alpha_{kl}^{'}dV)\sigma_{ij}^{0}\theta + \frac{1}{2}(\overline{c}_{p} + \frac{T_0}{V}\int_{V}\alpha_{ij}^{'}H_{ij}dV)\frac{\theta^2}{T_0} \tag{3.2.38}$$

which can be written in the same type of a bilinear form as that for the homogeneous material (3.2.33), that is

$$U_{\delta}^{C}(\sigma_{ij}^{0},\theta,\omega) = \frac{1}{2}S_{ijkl,\delta}(\omega)\sigma_{ij}^{0}\sigma_{kl}^{0} + \alpha_{ij\,\delta}(\omega)\sigma_{ij}^{0}\theta + \frac{1}{2}c_{p,\delta}(\omega)\frac{\theta^2}{T_0} \tag{3.2.39}$$

providing that the mesoscale properties are now identified as follows

$$\alpha_{ij,\delta}(\omega) = \bar{\alpha}_{ij} + \frac{1}{V}\int_V E_{ijkl}\alpha'_{kl}\,dV\,, \qquad c_{p,\delta}(\omega) = \bar{c}_p + \frac{T_0}{V}\int_V \alpha'_{ij}H_{ij}\,dV \tag{3.2.40}$$

Here we write explicitly that U^C is a functional of the applied stress σ^0_{ij}, the temperature increment θ, the actual realization of the microstructure $B(\omega)$, and the mesoscale δ.

3.2.4 Variational principles

Let us now recall from (Rosen & Hashin, 1970) that the variational principles in a thermoelastic problem can be stated in terms of potential and/or complementary energies. First, the variational principle in terms of the potential energy states that *of all the admissible displacement fields, those which satisfy the equilibrium equations make the potential energy minimum.* The minimum potential energy principle can be applied to an essential (Dirichlet) boundary value problem

$$U^e_P \le \tilde{U}^e_P \tag{3.2.41}$$

where $\tilde{U}^e_P$ is calculated for an admissible strain field (Christensen, 1979). Here we insert the superscript '*e*' on purpose so as to indicate the application of an essential boundary condition.

The variational principle in terms of the complementary energy states that *of all the admissible stress fields, those which satisfy the compatibility equation of strain make the complementary energy minimum.* This can be applied to a natural (Neumann) boundary value problem as follows,

$$U_C^n \le \tilde{U}_C^n \tag{3.2.42}$$

where $\tilde{U}_C^n$ denotes to an admissible stress field, and 'n' indicates a natural boundary condition.

Also, under the same kind of boundary condition, either natural or essential, we have $U_P^n = -U_C^n$ or $U_P^e = -U_C^e$, respectively.

3.3. Mesoscale Bounds on Thermal Effects

3.3.1 Scale dependent hierarchy on specific heat

Under the hypothesis of spatially homogeneous and ergodic statistics of material microstructure, we select an arbitrary realization $B_\delta(\omega)$ from the heterogeneous material space Ω. $B_\delta(\omega)$ is a square element for two dimensions and cubic element for three dimensions with nondimensional side length δ. We then consider partitioning of the window $B_\delta(\omega)$ of size δ into n^m subdomains (n = 2, 3,...; for the 2-D problem, m = 2; 3-D, m = 3), the subdomain with $B_{\delta'}^s(\omega)$ has the size $\delta' = \frac{\delta}{n}$, and s = 1, 2,..., n^m. We define two types of boundary conditions here — namely, the unrestricted and restricted boundary for $B_\delta(\omega)$ and $B_{\delta'}^s(\omega)$, respectively. Also, the body $B_\delta(\omega)$ is the union of all the constituent subdomains $B_{\delta'}^s(\omega)$

$$B_\delta(\omega) = \bigcup_{s=1}^{n^m} B^s_{\delta'}(\omega) \tag{3.3.1}$$

For simplicity, we set $n = 2$ and $m = 2$ for our particular partition in 2-D shown in Fig 2-1(b), and this can easily be extended to three dimensions and larger n.

First, under consideration are two essential boundary conditions: one of an unrestricted type

$$u_i(\vec{x}) = \varepsilon^0_{ij} x_j \quad \text{on} \qquad \partial B_\delta \tag{3.3.2}$$

and another of a restricted type

$$u_i(\vec{x}) = \varepsilon^0_{ij} x_j \quad \text{on} \qquad \partial B^s_{\delta'} \text{ ; s = 1,...,4} \tag{3.3.3}$$

We now observe that the solution under the restricted condition (3.3.3) on all four subdomains $B^s_{\delta'}(\omega)$ is an admissible solution with respect to the unrestricted condition (3.3.2) on $B_\delta(\omega)$, but not *vice versa.* Thus, in view of the principle of minimum potential energy, the following inequality is obtained

$$U^e_P(\delta) \ \leq \sum_{s=1}^{4} U^e_P(\delta')^r \tag{3.3.4}$$

The boundary condition (3.3.2) satisfies the Hill condition, so that, according to(3.2.31), the potential energy of the mesoscale domain under unrestricted and restricted boundary conditions can be written as follows

$$V_\delta \left(\frac{1}{2} C^e_{ijkl,\delta} \varepsilon^0_{ij} \varepsilon^0_{kl} + \Gamma^e_{ij} \varepsilon^0_{ij} \theta - \frac{1}{2} c^e_v \frac{\theta^2}{T_0}\right) \leq \sum_{s=1}^{4} V^s_{\delta'} \left(\frac{1}{2} C^e_{ijkl} \varepsilon^0_{ij} \varepsilon^0_{kl} + \Gamma^e_{ij} \varepsilon^0_{ij} \theta - \frac{1}{2} c^e_v \frac{\theta^2}{T_0}\right) \tag{3.3.5}$$

Here, and in the following, $C^e_{ijkl,\delta}$ is the apparent stiffness tensor for the *mesoscale* domain. [It is the subscript notation for the mesoscale tensor $\underline{\underline{C}}^e_\delta$ in symbolic notation, with ",δ" indicating the mesoscale, not a partial differentiation.] In the inequality (3.3.5) the elastic deformations and thermal effects are coupled. However, the case of zero temperature change θ reduces (3.3.5) to the well-known pure elasticity case

$$\left\langle C^e_{ijkl,\delta} \right\rangle \leq \left\langle C^e_{ijkl,\delta'} \right\rangle . \tag{3.3.6}$$

This then leads to the hierarchy of mesoscale stiffness tensors under essential boundary conditions bounding the RVE response from above

$$\underline{\underline{C}}^* \leq \cdots \leq \left\langle \underline{\underline{C}}^e_\delta \right\rangle \leq \left\langle \underline{\underline{C}}^e_{\delta'} \right\rangle \leq \cdots \leq \left\langle \underline{\underline{C}}^e_1 \right\rangle \qquad 1 < \delta' < \delta \tag{3.3.7}$$

On the other hand, setting the applied strain to zero ($\varepsilon^0_{ij} = 0$), leads to the inequality

$$V_\delta \left(-\frac{1}{2} c^e_v \frac{\theta^2}{T_0}\right) \leq \sum_{s=1}^{4} V^s_{\delta'} \left(-\frac{1}{2} c^e_v \frac{\theta^2}{T_0}\right) \tag{3.3.8}$$

Upon taking the ensemble average and noting the spatial homogeneity and ergodicity of the microstructure, we have $\left\langle c^e_{v,\delta} \right\rangle \geq \left\langle c^e_{v,\delta'} \right\rangle$. Since δ is selected arbitrarily, we arrive at the scale dependent hierarchy of volume specific heat under the essential boundary condition:

$$c^*_v \geq \cdots \geq \left\langle c^e_{v,\delta} \right\rangle \geq \left\langle c^e_{v,\delta'} \right\rangle \geq \cdots \geq \left\langle c^e_{v,1} \right\rangle \qquad 1 < \delta' < \delta \tag{3.3.9}$$

We now turn to the reciprocal expression for the lower bound. We shall now load the mesoscale domain through either one of two types of natural boundary conditions: one of an unrestricted type

$$t_i(\vec{x}) = \sigma_{ij}^0 n_j \qquad \text{on} \qquad \partial B_\delta \tag{3.3.10}$$

and another of a restricted type

$$t_i(\vec{x}) = \sigma_{ij}^0 n_j \quad \text{on} \quad \partial B_{\delta'}^s;\ \text{s} = 1,\ldots,4. \tag{3.3.11}$$

Considering the variational principle on complementary energy under both boundary conditions, an inequality similar to (3.4) can be obtained

$$U_C^n(\delta) \ \le \sum_{s=1}^{4} U_C^n(\delta')^r\ , \tag{3.3.12}$$

which, with reference to the Hill condition, leads to

$$V_\delta\left(\frac{1}{2}S_{ijkl,\delta}^n\sigma_{ij}\sigma_{kl} + \alpha_{ij}^n\sigma_{ij}\theta + \frac{1}{2}c_p^n\frac{\theta^2}{T_0}\right) \le \sum_{s=1}^{4} V_{\delta'}^s\left(\frac{1}{2}S_{ijkl}^n\sigma_{ij}\sigma_{kl} + \alpha_{ij}^n\sigma_{ij}\theta + \frac{1}{2}c_p^n\frac{\theta^2}{T_0}\right) \tag{3.3.13}$$

Again, for no thermal effects ($\theta = 0$), we arrive at the inequality $\left\langle S_{ijkl,\delta}^n \right\rangle \le \left\langle S_{ijkl,\delta'}^n \right\rangle^r$, under the natural boundary condition, which leads to the scale dependent hierarchy on the effective (RVE level) compliance tensor

$$\underline{\underline{S}}^* \le \cdots \le \left\langle \underline{\underline{S}}_\delta^e \right\rangle \le \left\langle \underline{\underline{S}}_{\delta'}^e \right\rangle \le \cdots \le \left\langle \underline{\underline{S}}_1^e \right\rangle \qquad 1 < \delta' < \delta \tag{3.3.14}$$

On the other hand, when $\sigma_{ij}^0 = 0$, we obtain

$$V_\delta\left(\frac{1}{2}c_p^n\frac{\theta^2}{T_0}\right) \le \sum_{s=1}^{4} V_{\delta'}^s\left(\frac{1}{2}c_p^n\frac{\theta^2}{T_0}\right) \tag{3.3.15}$$

After taking ensemble averages, we again have $\left\langle c^n_{p,\delta}\right\rangle \le \left\langle c^n_{p,\delta'}\right\rangle^r$ and this leads to the scale dependent hierarchy of pressure specific heat under the natural boundary condition as follows,

$$c^*_p \le \cdots \le \left\langle c^n_{p,\delta}\right\rangle \le \left\langle c^n_{p,\delta'}\right\rangle \le \cdots \le \left\langle c^n_{p,1}\right\rangle \qquad 1<\delta'<\delta \qquad (3.3.16)$$

This is the hierarchy of upper bounds on the pressure specific heat under the natural boundary condition (3.3.10). According to the hierarchies (3.3.9) and (3.3.16), we can see that the constitutive relation (3.2.10) does not hold unless the element size reaches the RVE size. Nevertheless, combining (3.2.10), (3.3.9) and (3.3.16) we obtain a hierarchy including both upper and lower bounds:

$$\begin{aligned}\left(\left\langle c^n_{P,1}\right\rangle - \left\langle T_0 C^n_{ijkl,1}\alpha^n_{ij,1}\alpha^n_{kl,1}\right\rangle\right) &\ge \left(\left\langle c^n_{P,\delta'}\right\rangle - \left\langle T_0 C^n_{ijkl,\delta'}\alpha^n_{ij,\delta'}\alpha^n_{kl,\delta'}\right\rangle\right) \ge \left(\left\langle c^n_{P,\delta}\right\rangle - \left\langle T_0 C^n_{ijkl,\delta}\alpha^n_{ij,\delta}\alpha^n_{kl,\delta}\right\rangle\right) \\ \ge \left(c^*_p - T_0 C^*_{ijkl}\alpha^*_{ij}\alpha^*_{kl}\right) = c^*_v \ge \cdots \ge \left\langle c^e_{v,\delta}\right\rangle \ge \left\langle c^e_{v,\delta'}\right\rangle \ge \left\langle c^e_{v,1}\right\rangle &\quad 1<\delta'<\delta \qquad (3.3.17)\end{aligned}$$

This hierarchy shows the upper and lower bound character on the effective specific heat and the scaling trend to RVE of both mesoscale bounds. In Section 4 a numerical simulation quantitatively demonstrates the convergence trends.

3.3.2 Scale effects on thermal expansion coefficient

We here consider the existence of scale dependent hierarchical bounds on thermal expansion coefficients. Unlike stiffness / compliance tensor and specific heat capacity under constant pressure/displacement, which follow similar kind hierarchical bounds with respect to the element scale (window size), thermal expansion coefficient bounds are different. It is noticed that the thermal expansion

coefficients appear non-quadratic term in the both energy formulations (3.2.33) and (3.2.39). These terms are coupled by elastic condition and temperature effects fully. Therefore, the hierarchical bound (convergence) on thermal expansion coefficients do not simply follow the upper/lower bounds under essential/natural boundary conditions. Even so, the uniqueness of the energy expression in (3.2.33) and (3.2.39) shows that there exists the convergence on the effective properties α_{ij}^{*} and Γ_{ij}^{*}. Combining them with elastic properties, we can still get the scale dependent relation on the thermal expansion coefficients.

We now consider a two-phase composite material. It was proved earlier (Christensen 1979) that, under the natural boundary condition (3.3.10) and by setting $P_{klmn}(S_{mnij}^{(1)} - S_{mnij}^{(2)}) = I_{klij}$, the thermal expansion coefficient can be expressed as

$$\alpha_{ij}^{n} = (\alpha_{kl}^{(1)} - \alpha_{kl}^{(2)}) P_{klmn}(S_{mnij}^{n} - S_{mnij}^{(2)}) + \alpha_{ij}^{(2)} \tag{3.3.18}$$

The derivation is detailed in Appendix B. Similarly, under the essential boundary condition (3.2), and by setting $P_{klmn}(C_{mnij}^{(1)} - C_{mnij}^{(2)}) = I_{klij}$, for the thermal stress coefficient we have

$$\Gamma_{ij}^{e} = (\Gamma_{kl}^{(1)} - \Gamma_{kl}^{(2)}) P_{klmn}(C_{mnij}^{e} - C_{mnij}^{(2)}) + \Gamma_{ij}^{(2)} \tag{3.3.19}$$

From the scale dependence of compliance and stiffness tensors (S_{mnij}^{n} and C_{mnij}^{n}) we can next derive the scale dependence of thermal expansion coefficients since P_{klmn} is scale independent by definition.

Considering each phase as isotropic and macroscopically isotropic composite, from (3.18) we have a simplified relation

$$\alpha_{ij}^{n} = (\alpha_2 - \alpha_1)\frac{1}{\left(1/\kappa_1 - 1/\kappa_2\right)}\left(S_{nnij}^{n} - \frac{\delta_{ij}}{\kappa_2}\right) + \alpha_2\delta_{ij} \tag{3.3.20}$$

where $S_{nnij}^{(n)}$ is the apparent (at mesoscale δ) compliance tensor under the natural boundary condition, $\kappa_1 and \kappa_2$ are bulk modulus for both phase respectively. Next, taking an ensemble average over (3.3.20), and noting the scale dependent hierarchy (3.3.14), leads to a scale dependent hierarchy on α_{ij}^{*}. In fact, we have two cases:

(i) $\alpha_1 > \alpha_2 \geq 0$ and $\kappa_1 > \kappa_2$:

$$\alpha^{*} \geq \cdots \geq \left\langle \alpha_{\delta}^{n} \right\rangle \geq \left\langle \alpha_{\delta'}^{n} \right\rangle \geq \cdots \geq \left\langle \alpha_{1}^{n} \right\rangle \quad 1 < \delta' < \delta \tag{3.3.21}$$

(ii) $\alpha_1 > \alpha_2 \geq 0$ and $\kappa_1 < \kappa_2$:

$$\alpha^{*} \leq \cdots \leq \left\langle \alpha_{\delta}^{n} \right\rangle \leq \left\langle \alpha_{\delta'}^{n} \right\rangle \leq \cdots \leq \left\langle \alpha_{1}^{n} \right\rangle \quad 1 < \delta' < \delta . \tag{3.3.22}$$

Using an expression for Γ_{ij}^{e} entirely analogous to (3.14)

$$\Gamma_{ij}^{e} = \frac{(\Gamma_1 - \Gamma_2)}{(\kappa_1 - \kappa_2)}\left(C_{nnij}^{e} - \delta_{ij}\kappa_2\right) - \Gamma_2\delta_{ij} \tag{3.3.23}$$

we derive hierarchical relations for these two cases:

(i) $0 \geq \Gamma_1 > \Gamma_2$ and $\kappa_1 > \kappa_2$:

$$\Gamma^{*} \leq \cdots \leq \left\langle \Gamma_{\delta}^{e} \right\rangle \leq \left\langle \Gamma_{\delta'}^{e} \right\rangle \leq \cdots \leq \left\langle \Gamma_{1}^{e} \right\rangle \qquad 1 < \delta' < \delta , \tag{3.3.24}$$

(ii) $0 \geq \Gamma_1 > \Gamma_2$ and $\kappa_1 < \kappa_2$:

$$\Gamma^* \geq \cdots \geq \left\langle \Gamma_\delta^e \right\rangle \geq \left\langle \Gamma_{\delta'}^e \right\rangle \geq \cdots \geq \left\langle \Gamma_1^e \right\rangle \qquad 1 < \delta' < \delta . \tag{3.3.25}$$

A closer inspection reveals that the case $\kappa_1 = \kappa_2$ does not present a singularity in (3.3.21~22) and (3.3.24~25). Note that since the Hill condition is satisfied on any mesoscale, we can use apparent properties in the constitutive relation (3.2.9) so as to arrive at upper and lower mesoscale bounds and scaling on RVE. The following numerical simulation results demonstrate the aforementioned bounds.

3.3.3 Legendre transformations

For a homogeneous continuum — or, equivalently, for a material homogenized at the RVE level - the complementary energy under traction prescribed boundary condition and the potential energy under displacement prescribed boundary are the negative of each other

$$U_P = -U_C \tag{3.3.25}$$

For a heterogeneous material below the RVE level — i.e. at the SVE level — the relation (3.2.15) does not hold. However, as shown in section 3.2.3, considering the spatial fluctuation terms in potential energy on one hand, and in the complementary energy on the other, one can write the Helmholtz and Gibbs energies in the following forms

$$A_\delta(\varepsilon_{ij}^0, \theta, \omega) = \frac{1}{2} C_{ijkl,\delta}(\omega) \varepsilon_{ij}^0 \varepsilon_{kl}^0 + \overline{\Gamma}_{ij,\delta}(\omega) \varepsilon_{ij}^0 \theta - \frac{1}{2} \overline{c}_{v,\delta}(\omega) \frac{\theta^2}{T_0} \tag{3.3.26}$$

and

$$G_\delta(\sigma_{ij}^0,\theta,\omega) = -\frac{1}{2}S_{ijkl,\delta}(\omega)\sigma_{ij}^0\sigma_{kl}^0 - \alpha_{ij,\delta}(\omega)\sigma_{ij}^0\theta - \frac{1}{2}\bar{c}_{p,\delta}(\omega)\frac{\theta^2}{T_0} \tag{3.3.27}$$

Under ensemble averaging, these become

$$\left\langle A_\delta(\varepsilon_{ij}^0,\theta)\right\rangle = \frac{1}{2}\left\langle C_{ijkl,\delta}\right\rangle\varepsilon_{ij}^0\varepsilon_{kl}^0 + \left\langle\overline{\Gamma}_{ij,\delta}\right\rangle\varepsilon_{ij}^0\theta - \frac{1}{2}\left\langle\bar{c}_{v,\delta}\right\rangle\frac{\theta^2}{T_0} \tag{3.3.28}$$

$$\left\langle G_\delta(\sigma_{ij}^0,\theta)\right\rangle = -\frac{1}{2}\left\langle S_{ijkl,\delta}\right\rangle\sigma_{ij}^0\sigma_{kl}^0 - \left\langle\alpha_{ij,\delta}\right\rangle\sigma_{ij}^0\theta - \frac{1}{2}\left\langle\bar{c}_{p,\delta}\right\rangle\frac{\theta^2}{T_0} \tag{3.3.29}$$

It follows that, under essential boundary conditions (ε_{ij}^0 controlled), the volume average stress is random (i.e. $\bar{\sigma}_{ij}(\omega)$), so that

$$G_\delta(\bar{\sigma}_{ij}(\omega),\theta) = A_\delta(\varepsilon_{ij}^0,\theta,\omega) - \bar{\sigma}_{ij}(\omega)\varepsilon_{ij}^0 \tag{3.3.30}$$

and hence, the ensemble average Gibbs energy on mesoscale δ should be calculated from $\left\langle A_\delta(\varepsilon_{ij}^0,\theta)\right\rangle$ according to

$$G_\delta(\left\langle\bar{\sigma}_{ij}\right\rangle,\theta) = \left\langle A_\delta(\varepsilon_{ij}^0,\theta)\right\rangle - \left\langle\bar{\sigma}_{ij}\right\rangle\varepsilon_{ij}^0 \tag{3.3.31}$$

rather than as $\left\langle G_\delta(\bar{\sigma}_{ij}(\omega),\theta)\right\rangle$.

Similarly, under natural boundary conditions (σ_{ij}^0 controlled), the volume average strain is random (i.e. $\bar{\varepsilon}_{ij}(\omega)$), so that

$$A_\delta(\bar{\varepsilon}_{ij}(\omega),\theta) = G_\delta(\sigma_{ij}^0,\theta,\omega) + \sigma_{ij}^0\bar{\varepsilon}_{ij}(\omega) \tag{3.3.32}$$

and hence, the ensemble average Gibbs energy on mesoscale δ should be calculated from $\left\langle A_\delta(\varepsilon_{ij}^0,\theta)\right\rangle$ according to

$$A_\delta(\left\langle \bar{\varepsilon}_{ij},\right\rangle\theta)=\left\langle G_\delta(\sigma_{ij}^0,\theta)\right\rangle+\sigma_{ij}^0\left\langle \bar{\varepsilon}_{ij}\right\rangle \tag{3.3.33}$$

rather than as $\left\langle A_\delta(\bar{\varepsilon}_{ij}(\omega),\theta)\right\rangle$.

When the mesoscale SVE reaches the RVE, the dependence on the type of boundary conditions vanishes, and we recover the classical relation for a homogeneous material (e.g. Houlsby & Puzrin, 2000)

$$A(\varepsilon_{ij},\theta)=G(\sigma_{ij},\theta)+\sigma_{ij}\varepsilon_{ij} \tag{3.3.34}$$

Here we simply write σ_{ij} and ε_{ij}. This, of course, is one pair out of all four possible Legendre transformations in a quartet linking the internal energy, Helmholtz free energy, enthalpy, and Gibbs energy. In a random medium, the relations (3.3.26-34) are special forms of that pair (Ostoja-Starzewski, 2002).

3.4 Numerical Simulations of Scaling Trends

3.4.1 Methodology

In order to demonstrate the hierarchies of bounds derived in Section 3, a series of numerical simulation is carried out on different mesoscales and under different boundary conditions. Our attention is focused on a planar (2-D), two-phase matrix-inclusion composite material with circular shaped inclusions. A finite element mesh, finer than the single inclusion, is employed in ABAQUS. The inclusion and matrix phases have different Young's moduli *E*, Poisson ratios

ν, thermal expansion coefficients α and specific heat c_p. In general, this leads to a characterization of the composite in terms of three mismatches (contrasts, or ratios of the inclusion property to the matrix property) E^i/E^m, ν^i/ν^m, α^i/α^m and c_p^i/c_p^m. Each realization is generated by a hard-core Poisson point field (Fig. 2-1(a)), with the inter-point distance being 1.2 times the disk diameter (so as to avoid the special problem of very narrow necks between the inclusions), and this process is repeated in a Monte Carlo sense to simulate an ensemble. The material properties and mismatches are listed in Table 1. Perfect bonding between inclusion and matrix phases is assumed.

Table 3-1 Material Properties of steel and aluminum

	E	ν	α	$c_p(J/g\cdot K)$
Aluminum	71*Gpa*	*0.3*	24×10^{-6}	*0.900*
Steel	211*Gpa*	*0.3*	12×10^{-6}	*0.452*
Mismatches	*3*	*1*	*0.5*	*0.5*

To compute all the hierarchies of Section 3, we proceed in the following steps:

(a) Choose a specific mesoscale δ and a nominal disk volume fraction;

(b) Generate a mesoscale realization $B_\delta(\omega)$ of the disordered medium;

(c) For a specific $B_\delta(\omega)$, apply the boundary condition (3.3.2) and compute the stiffness tensor $\underline{\underline{C}}_\delta^e(\omega)$, the thermal expansion stress coefficient $\underline{\Gamma}_\delta^e(\omega)$ and the constant-volume specific heat c_v numerically, Fig. 3.2.

Then the ensemble average is taken to compute the mesoscale bounds on the given mesoscale δ.

(d) For a specific $B_\delta(\omega)$, apply the boundary condition as (3.3.10) and can compute the compliance tensor $\underline{\underline{S}}^n_\delta(\omega)$, the thermal expansion strain coefficient $\underline{\alpha}^n_\delta(\omega)$ and the constant-pressure specific heat c_p on the given mesoscale δ.

(e) Proceed from (a) to (d) in a Monte Carlo sense over the sample space Ω so as to generate an ensemble of results at a fixed mesoscale δ: $\{\underline{K}_\delta(\omega);\omega\in\Omega\}$ and $\{\underline{R}_\delta(\omega);\omega\in\Omega\}$.

(f) Change the mesoscale and repeat steps (a) to (d) to find the first moments of all the mesoscale properties.

Fig. 3.1 and Fig. 3.2 demonstrate sample results on a very small mesoscale and a rather large mesoscale.

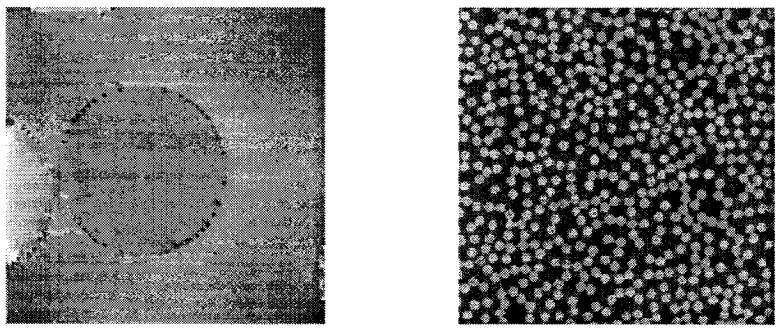

Fig. 3.1 Numerical results on $\delta = 2$ and $\delta = 32$ under the essential boundary condition (3.3.2) at $\varepsilon^0_{ij} = 0$.

In Fig. 3.2(a) for $\delta = 2$, the boundary deformation is very pronounced. On the other hand, for $\delta = 32$ in Fig. 3.2(b), the boundary deformation is hardly seen. Thus, we see the scaling trend from SVE towards the RVE. Since we deal with infinitesimal strains in linear thermoelasticity, in order to visualize the differences between responses under essential versus natural boundary conditions, displacements in these figures are plotted with an amplification factor of 200.

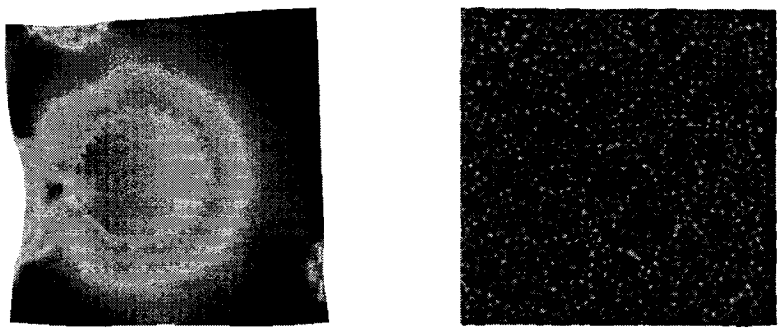

Fig. 3.2 Numerical results on $\delta = 2$ and $\delta = 32$ under the natural boundary condition (3.3.10) at $\sigma_{ij}^0 = 0$.

3.4.2 Numerical results

The hierarchy (3.3.9) states that the ensemble average of the specific heat under constant volume c_v increases when the mesoscale δ increases. Following the same methodology in computing permeability tensor in flow in porous media in chapter 2, we generate random realization sample sets with the increasing sample scale from $\delta = 2$ to $\delta = 32$ by the round disk inclusion model. Then we applied essential boundary condition $\varepsilon_{ij}^0 = 0$ in (3.3.2) and a temperature change θ on each samples and compute the specific heat c_v. This is brought out in Fig.

3-3 (a) that the ensemble average of c_v decreases with the increasing mesoscale. This demonstrates the hierarchical trend proved theoretically in (3.3.9).

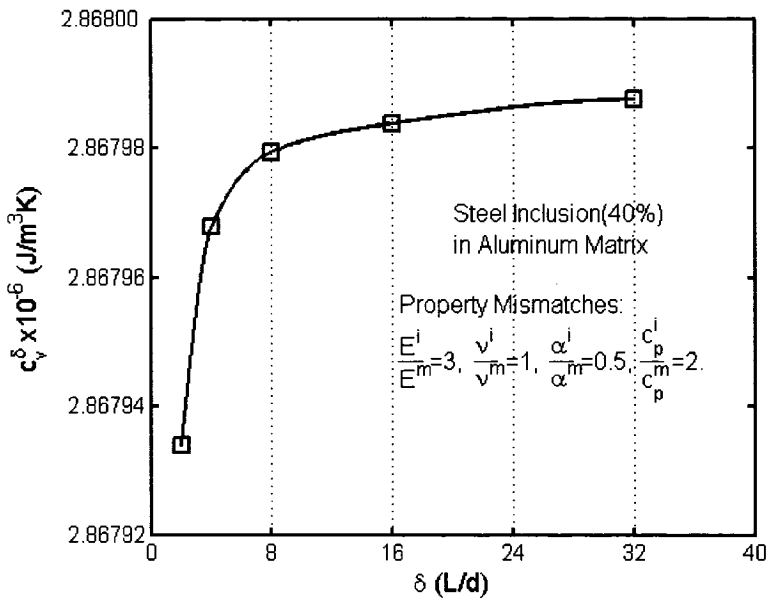

(a)

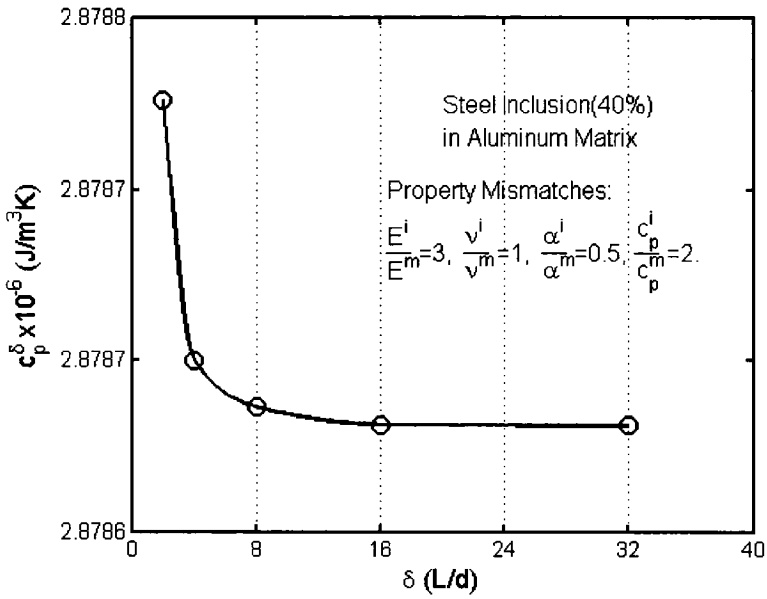

(b)

Fig. 3-3 Hierarchical trends for: (a) c_v under essential boundary condition $\varepsilon_{ij}^0 = 0$; (b) c_P under natural boundary condition $\theta_{ij}^0 = 0$.

On the other hand, we applied natural boundary condition $\sigma_{ij}^0 = 0$ and a temperature change θ on the same sample sets above. In such a way, the apparent $(c_p)_\delta^n$ were computed and the ensemble averages over different scales were taken. Fig 3-3 (b) shows that the ensemble average of c_P decreases with increasing δ. This demonstrates the theory of hierarchy (3.3.16).

All these results are combined in Fig. 3-4 after we applied constitutive relation (3.2.10). The specific heat $\langle c_v \rangle_\delta^n$ under natural boundary condition (note $\langle c_v \rangle_\delta^n$ is a computed value) were obtained and the convergence trend agrees the proof of the hierarchy (3.3.17). The ensemble average of specific heat under constant volume is bounded from below under essential boundary condition and from above by the value computed under natural boundary condition. These upper bound and lower bound come near to each other with the increasing mesoscale and will be equal at the size of RVE.

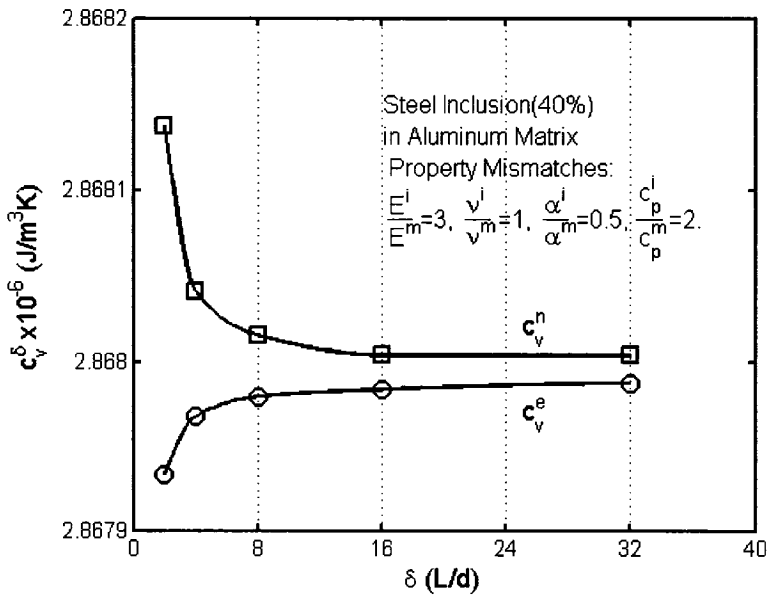

Fig. 3-4 Scaling of specific heat capacity from SVE towards RVE, shown in terms of upper and lower bounds.

For rather small mismatches in material properties chosen here, the numerical differences between $\langle c^e_{v,\delta} \rangle$ and $\langle c^n_{p,\delta} \rangle$ are (very) small, but the methodology developed here can be applied to study higher contrast materials.

Thermal expansion coefficients are also scale dependent due to their relation with the elastic properties stated in (3.3.18) and (3.3.19). We henceforth carry out numerical simulation to exhibit their scale dependent trends as per (3.3.21~22) and (3.3.24~25).

Similarly we applied natural boundary condition $\sigma^0_{ij} = 0$ and a temperature change θ on the sample sets at each mesoscale to compute thermal expansion strain coefficient α^n_{ij}. After taking ensemble average for each mesoscale, the trend of $\langle \alpha^n_{ij} \rangle_\delta$ vs. window scale is shown in Fig. 3-5. With reference to Table 1, we see that $\alpha_1 > \alpha_2 \geq 0$ and $k_1 < k_2$ so that the scale dependent trend on $\langle \alpha^n_{ij} \rangle$ follows the hierarchy (3.3.22).

Note in Table 3-1, we only provide Young's moduli and Poisson's ratio due to the requirement of ABAQUS. For isotropic phase, the bulk moduli can be calculated by

$$\kappa = \frac{E}{3(1-2\nu)} \tag{3.4.1}$$

As shown in Fig. 3-5(a), the ensemble average of $\langle \alpha^n_{ij} \rangle$ appears to decrease with the increasing mesoscale.

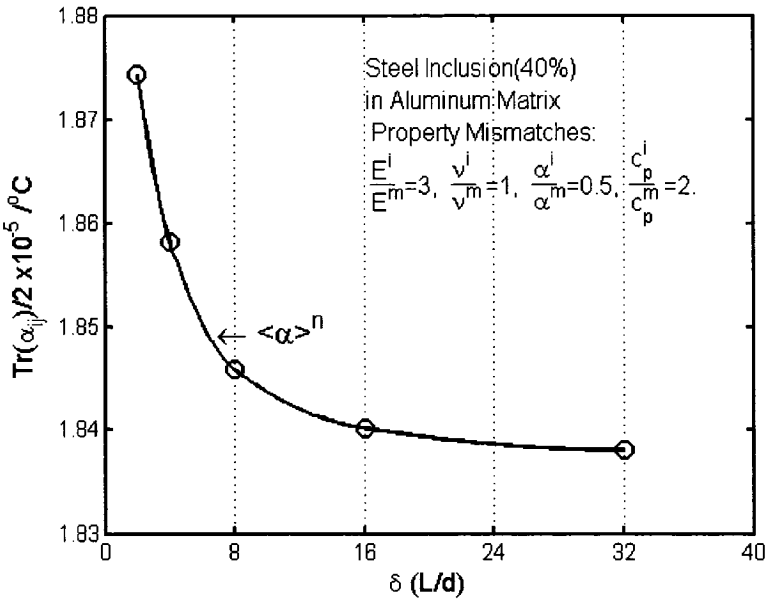

(a)

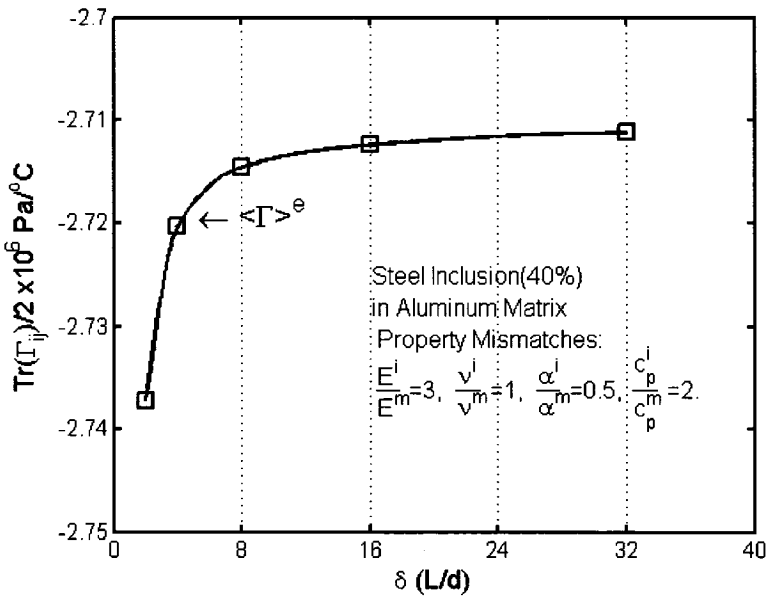

(b)

Figure 3-5 Numerical results on scale effects for the aluminum-steel composite of Fig. 1. (a) thermal strain coefficient under zero traction boundary condition (natural), (b) thermal stress coefficient under zero displacement boundary condition (essential)

On the other hand, considering the essential boundary condition $\varepsilon_{ij}^0 = 0$, the composite material model has the mismatches $0 \geq \Gamma_1 > \Gamma_2$ and $\kappa_1 > \kappa_2$. Here the thermal expansion stress coefficients of each isotropic material phase can be calculated by E and α as follows:

$$\Gamma = -3\kappa\alpha \tag{3.4.2}$$

Therefore, the scale dependent trend of $\langle \Gamma_{ij}^e \rangle$ must follow the hierarchy (3.3.24). Fig. 3-5(b) shows that the trace of $\langle \Gamma_{ij}^e \rangle$ increases with increasing mesoscale.

In order to obtain the convergence of $\langle \Gamma_{ij}^e \rangle$ and $\langle \alpha_{ij}^n \rangle$ towards the RVE, two separate hierarchical trends may not be sufficient to assess the size of RVE - both (upper and lower) mesoscale bounds are jointly necessary. Thus, we can apply equation (3.2.5) to set up bounds (upper and lower) in terms of essential and natural boundary conditions.

Fig. 3-6(a) shows numerical result on the upper and lower bounds for the trace of elastic stiffness tensor under essential and natural boundary conditions. Note here we used plane stress model and the engineering notation on compliance tensor and stiffness tensor. Consequently, modifying the formula (3.2.5) to $\Gamma_{ij}^n = -C_{ijkl}^n \alpha_{kl}^n$, and using the Legendre transformations of Section 3.3.3, the thermal stress coefficient corresponding to natural boundary condition is obtained at any given mesoscale. Fig. 3-6(b) shows that both the thermal stress coefficients under essential and natural boundary conditions converge toward each other when $\delta \to \infty$. At $\delta = 32$, the difference between Γ_{ij}^e and Γ_{ij}^n is less than 0.2%.

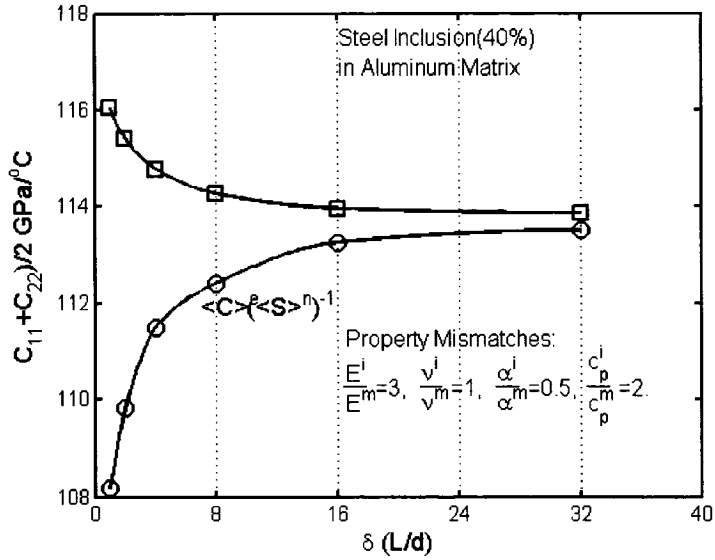

(a)

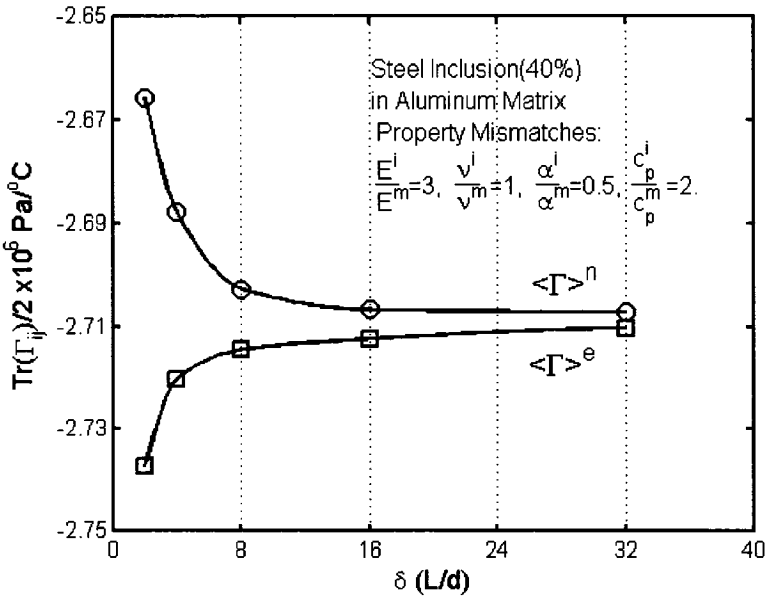

(b)

Fig. 3-6 Numerical results for the aluminum-steel composite of Fig. 1. (a) mesoscale bounds (upper and lower) on stiffness, (b) mesoscale bounds (upper and lower) on thermal stress coefficient.

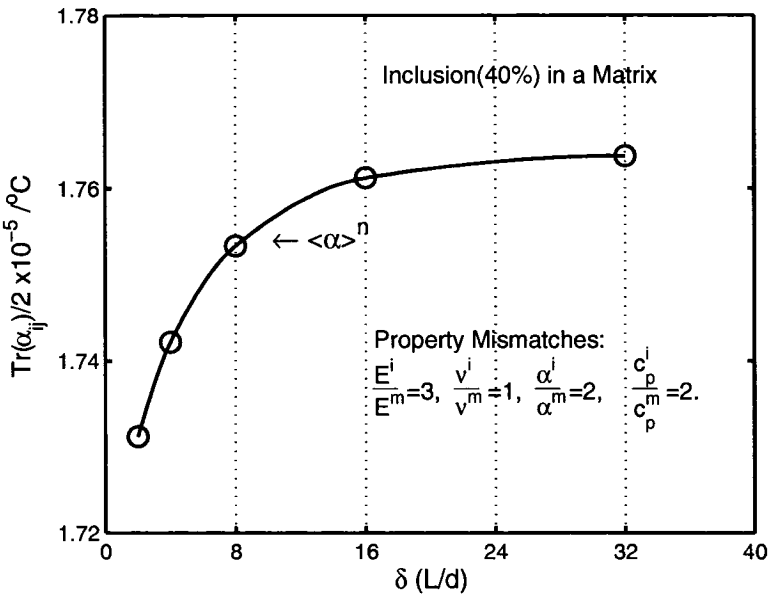

(a)

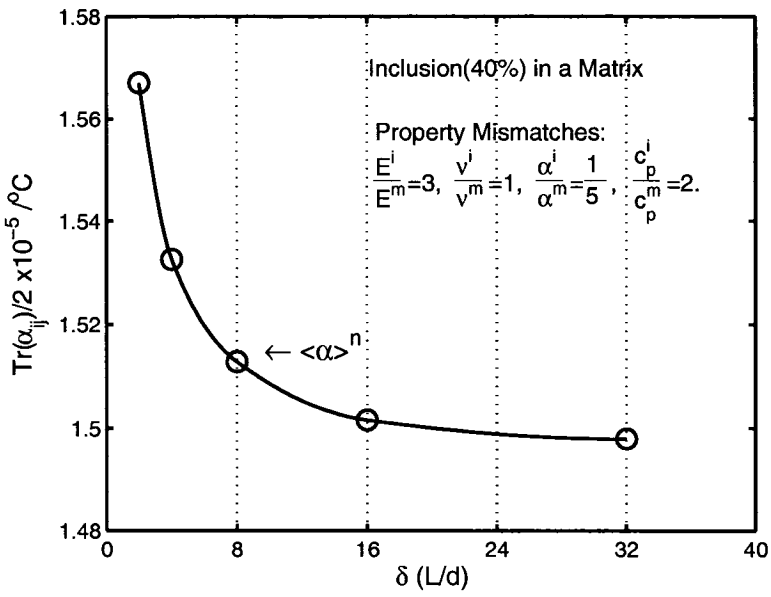

(b)

Fig. 3-7 Hierarchies of upper and lower bounds for two composite models (#1 and #2) of Section 4.2.2: (a) and (b) scale effects on thermal strain coefficients under zero traction boundary condition;

As stated in the derivation of (3.3.21~22) and (3.3.24~25), different mismatches in composites may present different hierarchical trends. We therefore

complete this paper with a study of two different kinds of composites having these mismatches:

$$\#1:\ \frac{E^i}{E^m}=3,\frac{\nu^i}{\nu^m}=1,\frac{\alpha^i}{\alpha^m}=2,$$

$$\#2:\ \frac{E^i}{E^m}=3,\frac{\nu^i}{\nu^m}=1,\frac{\alpha^i}{\alpha^m}=\frac{1}{5}.$$

In Fig. 3-7~9, these two 'opposite' cases of mismatches are compared using numerical simulations.

First we applied same computational procedure as in Figure 3-6(a) for case 1 and case 2 respectively. In particular, Fig. 3-7(a) shows that the composite possesses a hierarchical trend on α_{ij}^n according to (3.3.17), while Fig. 3-7(b) presents the trend according to (3.3.21).

Furthermore, we applied the same boundary condition as in Fig. 3.6(b) to compute $\langle \Gamma_{ij}^e \rangle$ for both cases. Note the Γ and κ of both phases were computed by (3.4.1) and (3.4.2). Case #1 has $\alpha_1 > \alpha_2$ and $\kappa_1 > \kappa_2$ such that we have $0 \geq \Gamma_2 > \Gamma_1$. Therefore we can see that Fig. 3-8(a) shows that $\langle \Gamma_{ij}^e \rangle$ increases with the increase of mesoscale which is proved in (3.3.25). On the other hand, Case #2 has $\alpha_1 < \alpha_2$ and $\kappa_1 > \kappa_2$. We computed Γ according to (3.3.2) such that we have $0 \geq \Gamma_1 > \Gamma_2$. We can see here that Fig. 3-8(b) shows the trend stated in (3.3.24).

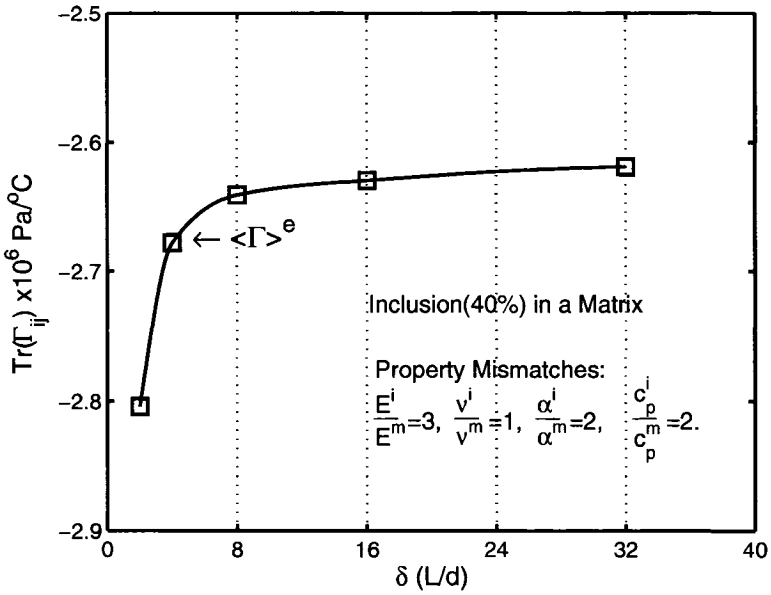

(a)

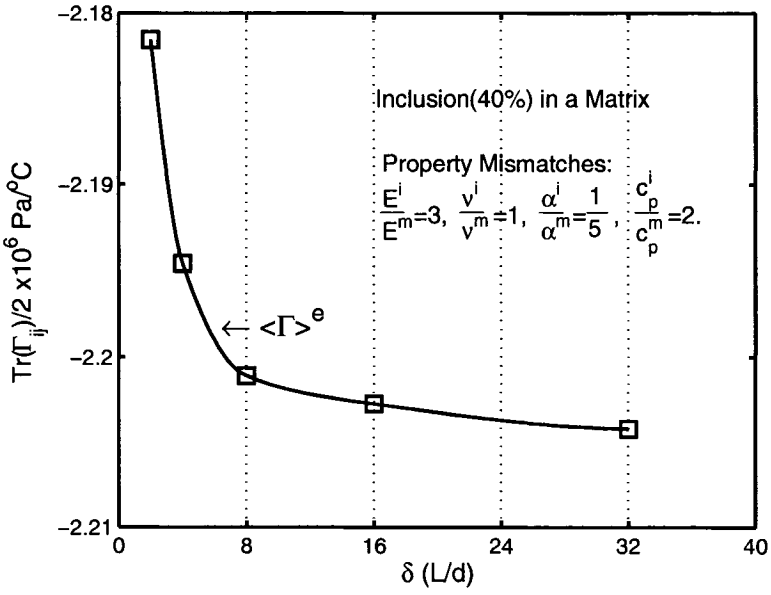

(b)

Fig. 3-8 Hierarchies of upper and lower bounds for two composite models (#1 and #2) of Section 4.2.2: (a) and (b) scale effects on thermal stress coefficients under zero displacement boundary condition.

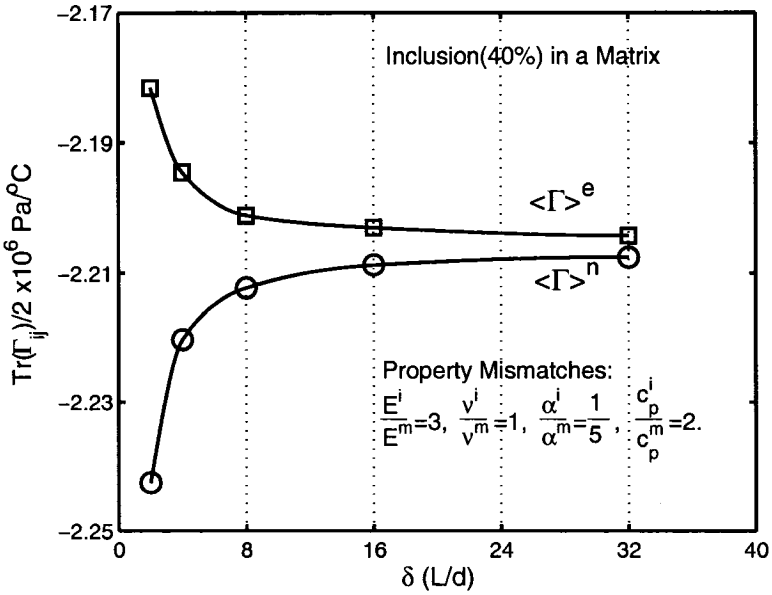

(a)

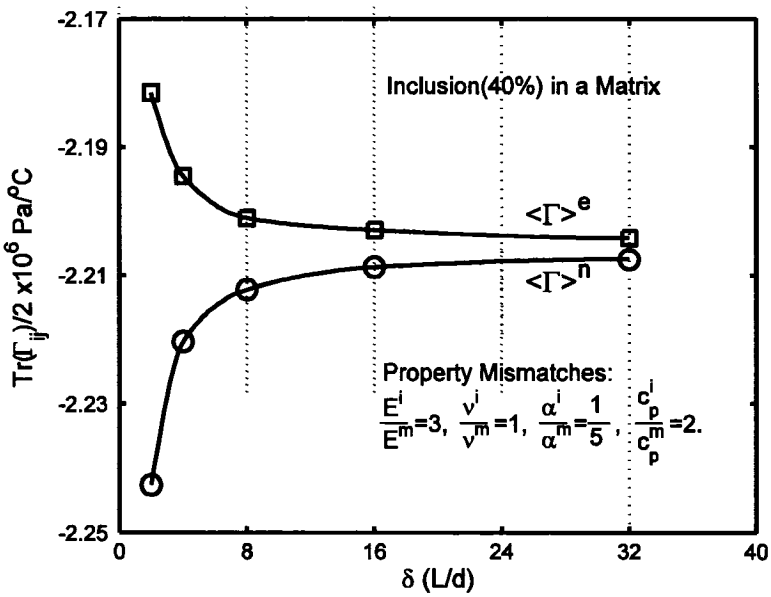

(b)

Fig. 3-9 Hierarchies of upper and lower bounds for two composite models (#1 and #2) of Section 4.2.2: (a) and (b) mesoscale bounds (upper and lower) on thermal stress coefficients.

Once again, employing the Legendre transformations of Section 3.3.3, we compute the upper and lower bounds presented in Figs. 3-9(a) and (b). In the case of the composite #1, the natural boundary condition provides the upper bound, while the essential boundary condition provides the lower bound. In contradistinction to this, in the case of the composite #2, the natural boundary condition gives the lower bound while the essential boundary condition gives the upper bound. In both cases, we clearly see that both bounds converge toward each other with the mesoscale increasing.

3.5. Conclusions

Results of this paper may be summarized as follows:

i) The Hill condition is extended so as to develop the equivalence between the energetic and mechanical formulations of constitutive laws of thermoelastic random heterogeneous materials at arbitrary mesoscale. Indeed, both energy forms (potential and complementary) of these materials can be cast in the same form as that of a homogeneous material (3.2.31) and (3.2.39).

ii) Using the variational principles, we obtain scale dependent hierarchies for the upper and lower bounds on the specific heat capacity at the RVE level. Application of essential (respectively, natural) boundary condition results in a hierarchy of lower bounds c_v^e (upper bounds

c_p^n). With increasing mesoscale, both bounds converge to one another in the sense that $c_p^* - c_v^* = T_0 C_{ijkl}^* \alpha_{ij}^* \alpha_{kl}^*$ is attained.

iii) Due to the presence of a non-quadratic term in energy formulas, the mesoscale bounds on the thermal expansion are more complicated than those on stiffness tensor and heat capacity. In general, upper and lower bounds correspond to loading of mesoscale domains by essential and natural boundary conditions. Depending on the property mismatches, the upper and lower bounds can be provided either by essential boundary condition or natural boundary conditions.

iv) In the proposed scale-dependent homogenization of thermoelastic properties, the RVE properties are attained approximately on a finite scale with whatever desired accuracy. In other words, the condition $d << L$ in the separation of scales (1.1) is not always necessary, and it is possible that the RVE is attained at $d < L$.

Chapter 4

Discussions and Future Work

In the present study on the mesoscale bounds of the apparent and effective properties of heterogeneous materials, the scale-dependent hierarchies on permeability of porous media flow were developed, as were the thermal expansion coefficients and specific heat for thermoelastic applications. It was shown that, in the sense of Hill, the general homogenization framework of the asymptotic approach can be summarized as follows:

(a) Formulate the energy functional (potential and complementary) in terms of the physical boundary conditions (essential and natural type);

(b) Establish the equivalence between the energetic approach and mechanical (physical) approach by invoking the Hill-Mandel type condition.

(c) Establish the variational principle in term of admissible solutions.

(d) Apply the partitioning method to obtain the mesoscale bounds.

(e) Obtain the scale dependent hierarchies for the material properties.

(f) Based on the constitutive relationship for the homogeneous material, construct the hierarchical relation between the different boundary conditions.

To homogenize the heterogeneous materials, this approach has been applied successfully in conductivity (thermal, electrical,...), the tangent moduli and strain energy in linear elasticity, heat transfer, elasto-plasticity, and nonlinear elasticity, respectively. In the present work, the approach has been extended to permeability

of random porous media and specific heats in thermoelasticity of random materials.

Regarding the first topic, due to the non-quadratic nature of the thermal expansion term in the energy formulation, the thermal expansion coefficient cannot be obtained using an energy formulation. Therefore, an alternative method is applied to derive the mesoscale bounds on thermal expansion coefficients. Boundary conditions of essential and natural types provide upper and lower bounds, respectively, and these converge toward the effective properties with the increasing mesoscale.

This study laid a theoretical foundation for engineering applications. The above procedures may also be applied in numerical and experimental laboratory studies. In the future, the present study may be extended to include the following:

1) More complicated models:

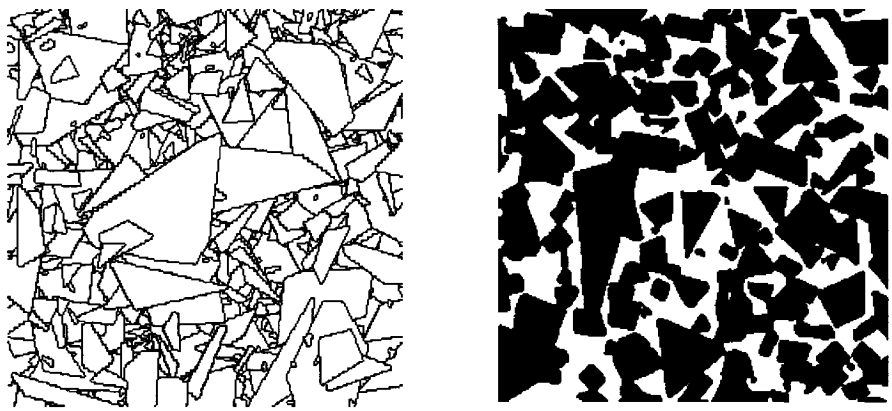

Figure 4.1 Microstructure of Random Material Models

In this study, the heterogeneous model is the round disk 2-phase material (Fig. 1.1). In most engineering problems, the geometry can be very different and more complex (Fig. 4.1).

Since no *a priori* assumptions were necessarily required regarding the specific geometry of the microstructure considered, except for the homogeneity and ergodicity of the spatial statistics, the convergence trends must follow the scale-dependent hierarchies which were derived in the above chapters. However, the rates of convergence can be different such that the RVE size differs with the microstructure type. Consequently, further study of the mesoscale bounds is required, especially for the case of materials in which the composites are anisotropic.

2) 3-D model

According to the previous studies (Huet, 1999; Ostoja-Starzewski 2001), 3-D models converge faster than 2-D ones. A typical 3-D model of a random sphere system is illustrated in Fig. 4.2. This model consists of random, spherical inclusions generated by a Poisson random process with inhibition. An extension of the methods presented in this thesis is being applied to this 3-D model as part of the ongoing research.

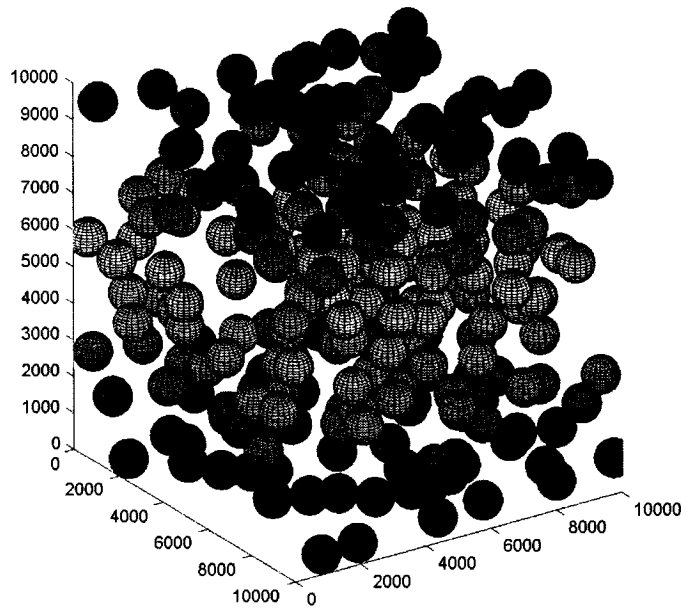

Figure 4.2 3-D random model of sphere inclusions

3) Discrepancy with respect to phenomena and mismatches of microstructures.

As the statement made above in (1.4), the size of the RVE is not necessary taken as 'very large'. In engineering applications, the finite separation scale may have certain errors. In Chapters 2 and 3, the discrepancies for the permeability and thermal expansion coefficient were presented.

In a recent comparative study (Ostoja-Starzewski *et. al.*, 2006), of which I am a co-author, the mesoscale size at $\delta = 16$ was studied for elasticity, thermal elasticity, plasticity, nonlinear elasticity and porous media flow. Table 4.1 shows the results of the composites with similar mismatches and the same geometry (Figure 4.3).

Table 4.1 Mismatch and discrepancy values (Ostoja-Starzewski et al 2006)

	Mismatch	Discrepancy [%]
Linear elasticity	$\frac{\mu^{(i)}}{\mu^{(m)}}=10, \frac{\kappa^{(i)}}{\kappa^{(m)}}=1$	2.28
Linear thermoelasticity	$\frac{\mu^{(i)}}{\mu^{(m)}}=10, \frac{\kappa^{(i)}}{\kappa^{(m)}}=10, \frac{\alpha^{(i)}}{\alpha^{(m)}}=\frac{1}{10}$	5.51
Plasticity	$\frac{h^{(i)}}{h^{(m)}}=10, \frac{E^{(i)}}{E^{(m)}}=1$	2.29
Nonlinear elasticity	$\frac{\mu_0^{(i)}}{\mu_0^{(m)}}=10, \frac{\kappa_0^{(i)}}{\kappa_0^{(m)}}=1$	5.86
Flow in porous media	$\frac{tr(\mathbf{K}^{(i)})}{tr(\mathbf{K}^{(m)})}=\infty$	27

The following conclusions can be drawn from the table:

(i) The discrepancy is increasing in the following order: linear elasticity, plasticity, linear thermoelasticity, and nonlinear elasticity.

(ii) By nature, the mismatch between solid and fluid phases in porous media is infinite, so the discrepancy value for permeability cannot be compared to the results in elasticity. The numerical results for this case show a discrepancy of 27% for the sample of size $\delta=16$, which obviously can not be considered homogeneous in the sense of Hill.

(iii) While in linear elasticity, the discrepancy is not a function of the strain, while in nonlinear elasticity it strongly depends on the deformation. Therefore, the value shown in Table 6.1 is the average over the considered deformation range.

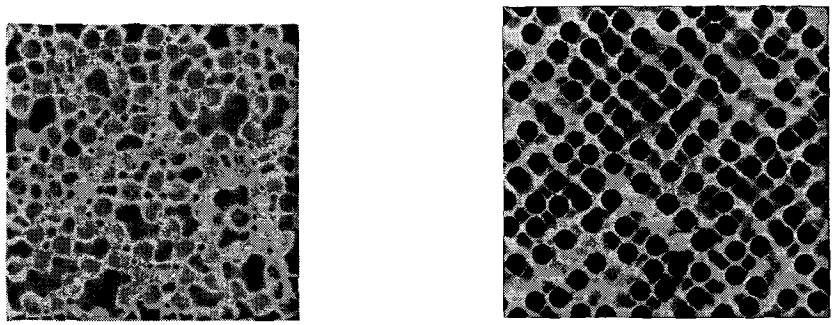

(a) (b)

Figure 4.3 Different phenomena of random materials of same realization: (a) thermal expansion field, (b) plastic field (Ostoja-Starzewski et al 2006). Note, the gray scale represents von-Mises strain.

Furthermore, the discrepancy can be used to evaluate the size of the RVE. The greater mismatches and more complex geometries should be investigated using the asymptotic approach methodology.

4) Experimental verification

The results presented in this work are based on theoretical derivations and numerical simulations. The methodology may also be applied to experimental and practical material tests. However, a number of challenges must first be addressed. First, the average sizes of the heterogeneities in different materials vary from the nanometer scale, up to meters, or even lager, so a nondimensional model must be developed. Therefore one may use the parameter $\delta = \frac{L}{d}$ as a basis for experimental tests and models. The second and most serious challenge is establishing appropriate experimental boundary conditions. As required by Hill (1963), the uniform boundary conditions (2.2.20~22, A4~6) are mandatory.

However, since the uniform boundary conditions are exceedingly difficult to apply experimentally (Juelin and Ostoja-Starzewski, 2000), the mixed boundary conditions offer the best connection with laboratory tests.

Appendix A

The Hill condition (1963) is a prerequisite for setting up the equivalence between the mechanical and energetic approaches to constitutive laws. In elasticity, along with the average strain/stress theorems, it provides the foundation for the mesoscale bounds for heterogeneous materials. To derive the Hill condition one starts from the equation

$$\overline{\sigma_{ij}:\varepsilon_{ij}}-\overline{\sigma_{ij}}:\overline{\varepsilon_{ij}}=\frac{1}{V}\int_V(\sigma_{ij}-\overline{\sigma_{ij}})\cdot(\varepsilon_{ij}-\overline{\varepsilon_{ij}})\,dV \tag{A.1}$$

Substituting the relation $\varepsilon_{ij}=u_{(i,j)}$ into (B.1), and then integrating by parts,

$$\begin{aligned}\overline{\sigma_{ij}:\varepsilon_{ij}}-\overline{\sigma_{ij}}:\overline{\varepsilon_{ij}}&=\frac{1}{V}\int_V(\sigma_{ij}-\overline{\sigma_{ij}})\cdot(u_{i,j}-\overline{u_{i,j}})\,dV\\&=\frac{1}{V}\int_V\{[(\sigma_{ij}-\overline{\sigma_{ij}})\cdot(u_i-\overline{u_i})]_{,j}-(\sigma_{ij,j}-\overline{\sigma_{ij,j}})\cdot(u_i-\overline{u_i})\}dV\end{aligned} \tag{A.2}$$

Considering the equilibrium condition $\sigma_{ij,j}=0$ in the absence of body and inertia forces, the second term inside the integral vanishes. Applying the Gauss-Green theorem to the first term, we obtain

$$\begin{aligned}\overline{\sigma_{ij}:\varepsilon_{ij}}-\overline{\sigma_{ij}}:\overline{\varepsilon_{ij}}&=\frac{1}{V}\int_{\partial V}(\sigma_{ij}-\overline{\sigma_{ij}})\cdot(u_i-\overline{u_i})n_j\,dS\\&=\frac{1}{V}\int_{\partial V}(\sigma_{ij}n_j-\overline{\sigma_{ij}}n_j)\cdot(u_i-\overline{u_i})\,dS\\&=\frac{1}{V}\int_{\partial V}(t_i-\overline{\sigma_{ij}}n_j)\cdot(u_i-\overline{\varepsilon_{ij}}x_j)\,dS\end{aligned} \tag{A.3}$$

Therefore, when the right side vanishes, we have $\overline{\sigma_{ij}:\varepsilon_{ij}}=\overline{\sigma_{ij}}:\overline{\varepsilon_{ij}}$ (i.e. the Hill condition (2.11)). This leads to three types of boundary conditions which satisfy the Hill condition:

1. uniform essential (Dirichlet) boundary condition:

$$u_i=\varepsilon^0_{ij}x_j \qquad \text{on } \partial B \tag{A.4}$$

2. uniform natural (Neumann) boundary condition:

$$t_i=\sigma^0_{ij}n_j \qquad \text{on } \partial B \tag{A.5}$$

3. uniform orthogonal-mixed boundary condition:

$$(t_i-\sigma^0_{ij}n_j)\cdot(u_i-\varepsilon^0_{ij}x_j)=0 \quad \text{on } \partial B \tag{A.6}$$

Appendix B

The follow part is based on Christensen (1979) in order to make a completed supplement for the derivation on the thermoelasticity.

We consider thermal expansion as the said that linear superposition by two boundary problems as follows,

$$t_i = \sigma_{ij}^0 n_j \text{ on } \partial V \text{ and } \theta = 0 \tag{B.1}$$

$$t_i = 0 \text{ on } \partial V \text{ and } \theta = \theta_0 \tag{B.2}$$

Following this we evaluate the product of stress and strain applying equilibrium equation $\sigma_{ij,i} = 0$. Then applying Gauss-Green theorem we can get,

$$\int_V \sigma_{ij}' \varepsilon_{ij} dv = \int_v (\sigma_{ij}' u_i)_{,j} dv = \int_S \sigma_{ij}' u_i n_j ds = \sigma_{ij}^0 \bar{\varepsilon}_{ij} V \tag{B.3}$$

In (B.2), the average strain theory can be written as $\bar{\varepsilon}_{ij} = \alpha_{ij}^{app} \theta_0$ such that

$$\int_V \sigma_{ij}' \varepsilon_{ij} dv = \sigma_{ij}^0 \alpha_{ij}^{app} \theta_0 V \tag{B.4}$$

In (B.4), we can define that,

$$\bar{\sigma}_{ij}' = \sum_{n=1}^{N} c_n \bar{\sigma}_{ij}'^{(n)} \tag{B.5}$$

To set up a certain transformation,

$$\bar{\sigma}_{ij}'^{(n)} = B_{ijkl}^{(n)} \sigma_{kl}^0 \tag{B.6}$$

Substituting (B.6) into (B.5),

$$\bar{\sigma}_{ij}' = \sum_{n=1}^{N} c_n B_{ijkl}^{(n)} \sigma_{kl}^0 \tag{B.7}$$

Due to average stress theorem,

$$\sum_{n=1}^{N} c_n B_{ijkl}^{(n)} = I_{ijkl} = \frac{1}{2}(\delta_{ik}\delta_{jl} + \delta_{il}\delta_{jk}) \tag{B.8}$$

Combining (B.7) and (B.4),

$$\alpha_{ij}^{app} = \sum_{n=1}^{N} c_n \alpha'^{(n)}_{ij} B_{ijkl}^{(n)} \tag{B.9}$$

By definition, we have

$$\bar{\varepsilon}'_{ij} = \sum_{n=1}^{N} c_n \bar{\varepsilon}'^{(n)}_{ij} \tag{B.10}$$

and

$$S_{ijkl}\sigma_{ij}^{0} = \sum_{n=1}^{N} c_n S_{ijkl} \bar{\sigma}'^{(n)}_{ij} \tag{B.11}$$

$$S_{ijkl}^{app} = \sum_{n=1}^{N} c_n S_{ijmn}^{(n)} B_{mnkl}^{(n)} \tag{B.12}$$

For material with two homogeneous phases, we can solve the problem.

$$c_2 B_{ijkl}^{(2)} = I_{ijkl} - c_1 B_{ijkl}^{(1)} \tag{B.13}$$

$$S_{ijkl} - S_{ijkl}^{(2)} = c_1 (S_{ijkl}^{(1)} - S_{ijkl}^{(2)}) B_{ijkl}^{(1)} \tag{B.14}$$

Set

$$P_{ijkl}(S_{ijkl}^{(1)} - S_{ijkl}^{(2)}) = I_{ijkl} \tag{B.15}$$

From (B.14) and (B.15) then,

$$P_{klmn}(S_{mnkl} - S_{mnkl}^{(2)}) = c_1 B_{klij}^{(1)} \tag{B.16}$$

Substituting into (B.9),

$$\alpha_{ij}^{n} = (\alpha_{kl}^{(1)} - \alpha_{kl}^{(2)}) P_{klmn}(S_{mnij}^{n} - S_{mnij}^{(2)}) + \alpha_{ij}^{(2)} \tag{B.17}$$

$$\alpha_{ij} = \alpha_n \delta_{ij}$$
$$S^{(n)}_{ijkk} = \frac{\delta_{ij}}{3k_n} \tag{B.18}$$

We can get $\alpha^n_{ij} = (\alpha_1 - \alpha_2)\delta_{kl} P_{klmn}(S^n_{mnij} - S^{(2)}_{mnij}) + \alpha_2 \delta_{ij}$ and $P_{kkmn} = \frac{3\delta_{mn}}{1/k_1 - 1/k_2}$,

$$\alpha_{ij} = (\alpha_2 - \alpha_1)\frac{1}{\left(1/k_1 - 1/k_2\right)}\left(S^{(n)}_{nnij} - \frac{\delta_{ij}}{k_2}\right) + \alpha_2 \delta_{ij} \tag{B.19}$$

Similarly,

$$\varepsilon_i = \varepsilon^0_{ij} n_j \text{ on } \partial V \text{ and } \theta = 0 \tag{B.20}$$

$$u_i = 0 \text{ on } \partial V \text{ and } \theta = \theta_0 \tag{B.21}$$

Following this we evaluate the product of stress and strain applying equilibrium equation $\sigma_{ij,i} = 0$. Then applying Gauss-Green theorem we can get,

$$\int_V \sigma_{ij}\varepsilon_{ij} dv = \int_v (\sigma'_{ij} u_i)_{,j} dv = \int_S \sigma'_{ij} u_i n_j ds = \bar{\sigma}_{ij} \varepsilon^0_{ij} V \tag{B.22}$$

In (B.2), the average strain theory can be written as $\bar{\sigma}_{ij} = \Gamma^{app}_{ij} \theta_0$ such that

$$\int_V \sigma'_{ij} \varepsilon_{ij} dv = \varepsilon^0_{ij} \Gamma^{app}_{ij} \theta_0 V \tag{B.23}$$

In (B.4), we can define that,

$$\bar{\varepsilon}'_{ij} = \sum_{n=1}^{N} c_n \bar{\varepsilon}'^{(n)}_{ij} \tag{B.24}$$

To set up a transformation,

$$\bar{\varepsilon}'^{(n)}_{ij} = B^{(n)}_{ijkl} \varepsilon^0_{kl} \tag{B.25}$$

Substituting (B.6) into (B.5),

$$\bar{\varepsilon}_{ij}^{'} = \sum_{n=1}^{N} c_n B_{ijkl}^{(n)} \varepsilon_{kl}^{0} \tag{B.26}$$

Due to average strain theorem,

$$\sum_{n=1}^{N} c_n B_{ijkl}^{(n)} = I_{ijkl} = \frac{1}{2}(\delta_{ik}\delta_{jl} + \delta_{il}\delta_{jk}) \tag{B.27}$$

Combining (B.7) and (B.4),

$$\Gamma_{ij}^{app} = \sum_{n=1}^{N} c_n \Gamma_{ij}^{(n)} B_{ijkl}^{(n)} \tag{B.28}$$

By definition, we have

$$\bar{\sigma}_{ij}^{'} = \sum_{n=1}^{N} c_n \bar{\sigma}'^{(n)}_{ij} \tag{B.29}$$

and

$$C_{ijkl}\varepsilon_{ij}^{0} = \sum_{n=1}^{N} c_n C_{ijkl} \bar{\varepsilon}'^{(n)}_{ij} \tag{B.30}$$

$$C_{ijkl}^{app} = \sum_{n=1}^{N} c_n C_{ijmn}^{(n)} B_{mnkl}^{(n)} \tag{B.31}$$

For material with two homogeneous phases, we can solve the problem.

$$C_{ijkl} - C_{ijkl}^{(2)} = c_1 (C_{ijkl}^{(1)} - C_{ijkl}^{(2)}) B_{ijkl}^{(1)} \tag{B.32}$$

Set

$$P_{ijkl}(C_{ijkl}^{(1)} - C_{ijkl}^{(2)}) = I_{ijkl} \tag{B.33}$$

From (B.14) and (B.15) then,

$$P_{klmn}(C_{mnkl} - C_{mnkl}^{(2)}) = c_1 B_{klij}^{(1)} \tag{B.34}$$

Substituting into (B.9),

$$\Gamma_{ij}^{n} = (\Gamma_{kl}^{(1)} - \Gamma_{kl}^{(2)}) P_{klmn}(C_{mnij}^{n} - C_{mnij}^{(2)}) + \Gamma_{ij}^{(2)} \tag{B.35}$$

$$\begin{aligned} \Gamma_{ij} &= \Gamma_n \delta_{ij} \\ C^{(n)}_{ijkk} &= 3k_n \delta_{ij} \end{aligned} \tag{B.36}$$

We can get $\alpha^n_{ij} = (\alpha_1 - \alpha_2)\delta_{kl} P_{klmn}(S^n_{mnij} - S^{(2)}_{mnij}) + \alpha_2 \delta_{ij}$ and $P_{kkmn} = 3\delta_{mn}(k_1 - k_2)$,

$$\alpha_{ij} = (\alpha_2 - \alpha_1)\frac{1}{\left(1/k_1 - 1/k_2\right)}\left(S^{(n)}_{nnij} - \frac{\delta_{ij}}{k_2}\right) + \alpha_2 \delta_{ij} \tag{B.37}$$

References

1. Adler, P. M., Jacquin, C. G. and Quiblier, J. A. (1990), FLOW IN SIMULATED POROUS MEDIA, *Int. J. Multiphase Flow*, Vol. 16, No. 4, pp. 691-712

2. Beasley, J. D. and Torquato, S. (1988), New bounds on the permeability of a random array of spheres, *Physics of Fluids A*, Vol. 1, No. 2, pp. 199-207.

3. Beran, M.J. (1968), *Statistical Continuum Theories*, J. Wiley & Sons.

4. Berryman, J.G. & Milton, G.W. 1985 Normalization constraint for variational bounds on fluid permeability, J. Chem. Phys. 83 (2), 754-760.

5. Cheng, Z. Q. and Batra, R. C. (2000), Three-dimensional thermoelastic deformations of a functionally graded elliptic plate, *Composites Part B: Engineering*, Volume 31, Issue 2, pp. 97-106.

6. Childress, S. (1972), Viscous Flow Past a Random Array of Spheres, *Journal of Chemical Physics*, Vol. 56, pp.2527.

7. Christensen, R.M. (1979), *Mechanics of Composite Materials*, J. Wiley & Sons.

8. Chung, T.J. 2000 Computational Fluid Dynamics, Cambridge University Press.

9. Du, X. & Ostoja-Starzewski, M. (2005), Mesoscale bounds on effective thermal expansion of random composites, *Proc. 20th CANCAM*, 463-464, Montréal, Canada.

10. Dullien, F.A.L. 1979 Porous Media: Fluid Transport and Pore Structure, Academic Press.

11. Eshelby, J. D. (1957), The determination of the elastic field of an ellipsoidal inclusion and related problems, *Proceedings of Royal Society of London A*, Vol. 241, pp. 376-396.

12. Hazanov, S. (1998), On apparent properties of nonlinear heterogeneous bodies smaller than the representative volume, *Acta Mech.* **134**, 123-134.

13. Hill, R. (1963), Elastic properties of reinforced solids: Some theoretical principles. *J. Mech. Phys. Solids* **11**, 357-372.

14. Hill, R. and Koch, D. (2001), Moderate-Reynolds-number flows in ordered and random arrays of spheres, *Journal of Fluid Mechanics*, vol. 448, pp. 243-278.

15. Howells, I. D. (1974), Drag due to the motion of a Newtonian fluid through a sparse random array of small fixed rigid objects, *Journal of Fluid Mechanics*, Vol. 64, 449.

16. Huet, C., (1990), Application of variational concepts to size effects in elastic heterogeneous bodies, *J. Mech. Phys. Solids* **38**, 813-841.

17. Huet, C. (1999), Coupled size and boundary-condition effects in viscoelastic heterogeneous and composite bodies, *Mech. Mater.* **31**(12), 787-829.

18. Jacob, Bear (1988), *Dynamics of Fluids in Porous Media*, Courier Dover Publications.

19. Juelin, D. and Ostoja-Starzewski, M. (2001), *Mechanics of Random and Multiscale Microstructures*, Springer.

20. Kanit, T. and Forest, S., Galliet, I., Monoury, V. and Jeulin, D. 2003 Determination of the size of the representative volume element for random composites: statistical and numerical approach, Int. J. Solids Struct. 40, 3647-3679.

21. Khisaeva, Z. & Ostoja-Starzewski, M. (2005), Mesoscale bounds in finite elasticity and thermoelasticity of random composites, submitted to Proc. Roy. Soc. Lond. A.

22. Kitanidis, P. K. and Dykaar, B. B. (1997), Stokes Flow in a Slowly Varying Two-Dimensional Periodic Pore, *Transport in Porous Media*, Vol. 26: 89–98.

23. Koch, D. and Ladd, A. (1997), Moderate Reynolds number flows through periodic and random arrays of aligned cylinders, *Journal of Fluid Mechanics*, Vol. 349, pp. 31-66, Cambridge University Press.

24. Love, A. E. H. (1926), *A Treatise on the Mathematical Theory of Elasticity*, 4th Edition, Dover Publication, New York.

25. Markov, K. Z. & Preziosi, L. (2000), *Heterogeneous Media*, Birkhäuser, Basel.

26. Martys, N., Bentz, D. P., and Garboczi, E. J. (1994), Computer simulation study of the effective viscosity in Brinkman's equation, *Physics of Fluids*, Vol. 6, No. 4, pp1436-1439.

27. Milton, G.W. (2002), *Theory of Composites*, Cambridge University Press.

28. Mura, T. (1987). *Micromechanics of Defects in Solids*, Second, Revised Edition, Kluwer Academic Pub.

29. Lemaitre, J. & Chaboche, J.-L. (1994), *Mechanics of Solid Materials*, Cambridge University Press.

30. Nemat-Nasser, S. & Hori, M. (1993), *Micromechanics: Overall Properties of Heterogeneous Solids*, North-Holland, Amsterdam.

31. Nadeau, J. C., and Ferrarib, M. (2004), Effective thermal expansion of heterogeneous materials with application to low temperature environments, *Mechanics of Materials*, Vol. 36, Issue 3, pp. 201-214.

32. Ostoja-Starzewski, M. (1994) Micromechanics as a basis of continuum random fields, *Appl. Mech. Rev.* (Special Issue: *Micromechanics of Random Media*) **47**(1, Part 2), S221-S230.

33. Ostoja-Starzewski, M. and Schulte, J. (1996), Bounding of effective thermal conductivities by essential and natural boundary conditions, Phys. Rev. B 54, 278-284.

34. Ostoja-Starzewski, M. (1998), Random field models of heterogeneous materials, *International Journal of Solids and Structures*, Volume **35**, Issue 19, Pages 2429-2455

35. Ostoja-Starzewski, M. (2001), Mechanics of random materials: Stochastics, scale effects, and computation, in *Mechanics of Random and*

Multiscale Microstructures (Eds. D. Jeulin & M. Ostoja-Starzewski), *CISM Courses and Lectures* **430**, Springer-Wien-New York, 93-161.

36. Ostoja-Starzewski, M. (2002), Towards stochastic continuum thermodynamics, *J. Non-Equilib. Thermodynamics* **27**(4), 335-348.

37. Ostoja-Starzewski, M. (2005), Scale effects in plasticity of random media: Status and challenges, *Int. J. Plasticity* **21**, 1119-1160.

38. Ostoja-Starzewski, M. & Wang, C. (1989), Linear elasticity of planar Delaunay networks: Random field characterization of effective moduli, *Acta Mech.* **80**, 61-80.

39. M. Ostoja-Starzewski, X. Du, Z.F. Khisaeva and W. Li (2006), On the Size of Representative Volume Element in Elastic, Plastic, Thermoelastic and Permeable Random Microstructures. *THERMEC'2006*, Vancouver.

40. Patankar, S.V. 1980 Numerical Heat Transfer and Fluid Flow, McGraw-Hill.

41. Prager, S. 1961 Viscous flow through porous media, Phys. Fluids 4, 1477-1482.

42. Poutet, J., Manzoni, D., Hage-Chehade, F., Jacquin, C.J., Bouteca, M.J., Thovert, J.-F., Adler, P.M. (1996), The effective mechanical properties of random porous media, *Journal of the Mechanics and Physics of Solids*, Vol. 44, Number 10, pp.1587-1620.

43. Rosen, B.W. & Hashin, Z. (1970), Effective thermal expansion coefficient coefficients and specific heats of composite materials, *Int. J. Engng. Sci.* **8**, 157-173.

44. Rubinstein, J. & Torquato, S. (1989), Flow in random porous media: mathematical formulation, variational principles, and rigorous bounds, J. Fluid. Mech. 206, 25-46.

45. Sab, K. (1992), On the homogenization and simulation of random materials, Eur. J. Mech. A/Solids, 11(5), 585-607.

46. Sab, K. (1991), Principe de Hill et homogénéisation des matériaux aléatoires, C. R. Acad. Sci. Paris II 312, 1-5.

47. Shapery, R. A. (1968), Thermal expansion coefficients of composite materials, based on energy principles, *J. Compos. Mat.*, vol. 2, pp.380–404.

48. Sigmund, O. and Torquato, S. (1996) Composites with extremal thermal expansion coefficients, Applied Physics Letters, Vol. 61(21), pp. 3203-3205.

49. Torquato, S. (2002), Random Heterogeneous Materials: Microstructure and Macroscopic Properties, Springer-Verlag, Berlin-New York.

50. Weissberg, H.L. and Prager, S. (1962), Viscous Flow through Porous Media. II. Approximate Three Point Correlation Function, *Physics of Fluids*, Vol. 5, No. 11, pp. 1390-1392.

51. Zhang, Dongxiao (2001), *Stochastic Methods for Flow in Porous Media: Coping with Uncertainties*, Elsevier.

52. Ziegler, H. (1983), *An introduction to thermomechanics*. Amsterdam: North-Holland.

53. Ziegler & Wehrli, (1987), The derivation of constitutive relations from the free energy and the dissipation function, *Advances in Applied Me*chanics, Vol. 25, pp.183-238, Academic Press.

54. Zick. A, and G. Homsy (1982), Stokes flow through periodic arrays of spheres, *Journal of Fluid Mechanics*, Vol. 115, pp.13-26, Cambridge University Press.